Title

LEVELS OF 2o8Po FROM RADIOACTIVE DECAY AND MJCLEAR REACTION -RAY SPECTROSCOPY

Authors

Treytl, William J.
Hyde, Earl K.
Yamazaki, Toshimitsu.

Publication Date

1968-04-01

UCRL-17529

University of California
Ernest O. Lawrence
Radiation Laboratory

LEVELS OF ^{208}Pb FROM RADIOACTIVE DECAY AND NUCLEAR REACTION γ-RAY SPECTROSCOPY

William J. Treytl, Earl K. Hyde, and Toshimitsu Yamazaki

April 1968

DISCLAIMER

to be submitted to Nuclear Physics

UCRL-17529
Preprint

UNIVERSITY OF CALIFORNIA

Lawrence Radiation Laboratory
Berkeley, California

AEC Contract No. W-7405-eng-48

LEVELS OF ^{208}Po FROM RADIOACTIVE DECAY AND NUCLEAR REACTION γ-RAY SPECTROSCOPY

William J. Treytl, Earl K. Hyde, and Toshimitsu Yamazaki

April 1968

LEVELS OF ^{208}Po FROM RADIOACTIVE DECAY AND NUCLEAR REACTION γ-RAY SPECTROSCOPY*

William J. Treytl†, Earl K. Hyde, and Toshimitsu Yamazaki‡

Lawrence Radiation Laboratory
University of California
Berkeley, California

April 1968

Abstract

Information obtained from a study of the radioactive decay of 1.7 hour ^{208}At and from on-line studies of the γ-radiations emitted by ^{208}Po produced in ^{209}Bi(p,2n), ^{206}Pb(α,2n), and ^{208}Pb(α,4n) reactions has been used to construct a decay scheme for ^{208}At and a level scheme for ^{208}Po. Many of the low-lying levels can be explained on the basis of the known levels of ^{206}Pb and ^{210}Po and the weak coupling approximation. Among the interesting features of the scheme is a 380 nanosecond state which is identified as the 8+ member of the band of levels resulting from the proton configuration $(h_{9/2})^2$.

RADIOACTIVITY: ^{208}At; measured $E_\gamma E_{el}$ $\gamma T_{1/2}$ I_γ γ γ coin. ^{208}Po deduced levels $J\pi$.

NUCLEAR REACTIONS: ^{209}Bi(p,2n), ^{206}Pb(α,2n), ^{208}Pb(α,4n) measured E_γ γ lifetimes γ angular distribution.

1. Introduction

The purpose of this work was to study the level scheme of ^{208}Po, a nucleus which is of some theoretical interest owing to its proximity to ^{208}Pb. It has two protons more than a closed shell of 82 and two neutrons less than a closed configuration of 126. One might hope to understand its level structure by a shell model description. As a first approximation one might start from the level schemes of ^{210}Po and ^{206}Pb, about which much is known, and apply the weak coupling approximation to describe the interaction of the two neutron hole states with the two proton states.

Our first approach to the experimental goal of this paper was a detailed study of the radiations emitted by 1.7-hour ^{208}At in its electron capture decay to ^{208}Po. Gamma ray energies and intensities were measured with lithium-drifted germanium detectors and conversion electrons were studied with silicon semiconductor detectors. Additional information was obtained by prompt and delayed coincidence techniques. Valuable additional information was obtained by the study of ^{208}Po radiations emitted during the course of ^{209}Bi(p,2n)^{208}Po and ^{206}Pb(α,2n)^{208}Po reactions carried out at the Berkeley 88-inch cyclotron. These measurements were made with germanium detectors placed near the target at the cyclotron. The characteristics of the beam and of the counting equipment were such that the ^{208}Po gamma rays could be analyzed on a nanosecond time scale during and between cyclotron beam bursts.

Astatine-208 was first reported by Hyde, Ghiorso, and Seaborg[1]) who observed its formation by the α-decay of 19-minute ^{212}Fr and reported a half life of 1.7 hours and an EC/α branching ratio of 200. The product of electron capture decay is 2.93-year ^{208}Po. Astatine-208 can also be prepared by bombardment of bismuth with high energy alpha particles, but other astatine

isotopes of similar half life are prepared at the same time. Studies of astatine prepared in this way seemed to suggest[2] the occurrence of isomeric forms of ^{208}At with half lives of 1.7 and 6.3 hours, but later work by Thoresen, Asaro, and Perlman[3] disproved the existence of the 6.3-hour form. The only attempt to measure the radiations of ^{208}At was made in a 1956 thesis study by Stoner[4] who used NaI detectors to measure the γ rays. He reported prominent γ rays at 175 and 660 keV in coincidence plus some evidence for a γ ray at 250 keV.

In the experimental section to follow we first present the results of our restudy of ^{208}At decay and then the results of in-beam measurements of ^{208}Po radiations as produced in the $Bi^{209}(p,2n)^{208}Po$, $^{206}Pb(\alpha,2n)$, and $^{208}Pb(\alpha,4n)$ reactions. In section 3 we present a ^{208}Po level scheme and discuss the evidence for this scheme on a level-by-level basis. We conclude in section 4 with a discussion of a possible interpretation of the results.

2. Experimental

2.1. ASTATINE-208 SAMPLE PREPARATION

Having decided to restudy ^{208}At we considered all possible ways of preparing it and decided on the following as the most suitable for preparation of radioactivity-pure samples. We bombarded thick targets of metallic thallium with 120 MeV ^{12}C ions in the Berkeley Heavy Ion Linear Accelerator (HILAC) to produce 19.3-minute ^{212}Fr by the reaction $^{205}Tl(^{12}C,5n)^{212}Fr$. Francium was separated in carrier-free form from the one gram thallium target and from radioactive reaction products by techniques fully described elsewhere[5]. In its essentials the technique involved the coprecipitation of tracer francium on

silicotungstic acid precipitated from cold saturated HCl solution, followed by the dissolution of the precipitate in water, the adsorption of the francium on a short ion-exchange column of Dowex 50 resin, and later desorption of the activity with 6M hydrochloric acid. The time taken for the separation ranged from 40 to 60 minutes so that all francium isotopes shorter-lived than ^{212}Fr had decayed to a negligible level.

In some experiments aliquots of the final ^{212}Fr sample were used without further treatment for the measurements of ^{208}At radiations about 1 or 2 hours after preparation or, more usually, after an hour's decay of ^{212}Fr, the ^{208}At daughter was extracted from the 6M HCl solution into di-isopropyl ether which was washed with 6-8M HCl and then evaporated to make the final ^{208}At samples. Samples prepared in this way showed no evidence of contamination with any radioactive nuclide.

2.2. GAMMA SPECTROSCOPY—ASTATINE-208 SINGLES SPECTRA

Gamma radiations were measured with several semiconductor detectors. Most measurements were made with a 6 cm^2 × 8 mm deep lithium-drifted germanium detector. We also used a large coaxially drifted detector with a sensitive volume of 32 cc. All detectors were made by the semiconductor detector group of this laboratory. Conventional electronic circuitry was used throughout and spectra were recorded on commercial multi-channel analyzers. The efficiency and geometry factors for all detectors were measured as a function of γ-energy with a series of calibrated gamma sources. Spectra were taken repeatedly over a period of several ^{208}At half lives to establish that all observed γ rays belonged to the same isotope.

Figure 1 shows the γ-region from 90 to 1100 keV as recorded by the 6 cm^2 × 8 mm deep detector in three consecutive measurements separated by about 2 hours. Figure 2 shows the entire spectrum from 177 to 3000 keV as recorded by the 30 cc detector. Figure 3 shows the low energy region from 10 keV to 100 keV recorded in a third detector, a thin silicon detector of dimensions 3 cm^2 with a 3 mm sensitive depth. This detector used an electronic system with a cooled field-effect transistor as the first stage of a charge sensitive preamplifier[6]). The energy resolution of this system was 0.7 keV full-width-at-half-maximum for X rays and γ rays in the 0-150-keV range, and hence, was well suited for the search for γ-transitions in this energy range.

The gamma rays detected in these and similar measurements are listed in table 1 together with relative intensities and other information. The most intense γ rays have energies 177, 660, and 685 which, as we shall see below, form a triple cascade which appears in a majority (79%) of the decay events. Other gamma rays, in intensity greater than 5%, occur at 206, 517, 808, 845, 896, 986, 993, and 1028 keV.

2.3. CONVERSION COEFFICIENT MEASUREMENTS

Some conversion coefficients were made in a conversion coefficient spectrometer constructed by Easterday, Haverfield, and Hollander[7]). This instrument consisted of a Ge(Li)γ detector (4 cm^2 × 0.5 mm) and a silicon semiconductor electron detector (1 cm^2 × 3 mm) mounted in an evacuated metal box in fixed geometric positions with respect to the sample location. The combined geometry and efficiency factors of both crystals were measured as a function of radiation energy with a series of standards[7]). A sample of

Table 1

^{208}Po γ rays seen in ^{209}Bi(p,2n)^{208}Po reactions (keV)	^{208}Po γ rays seen in ^{208}At decay (keV)	Relative transition Intensity $I_\gamma + I_e$ (in percent)† for ^{208}At decay	Conversion Electrons Observed	Multipolarity
	11.1 Lα			
	13.3 Lβ			
	15.5 Lγ			
	77.0 Kα2 X rays			
	79.4 Kα1			
	89.9 Kβ1			
	92.4 Kβ2			
149.8	148	< 0.5		
177	177	79	K,L,M	E2
206	206	12	K,L,M	M1
	252*	< 0.5	L	
	332*	< 0.5	K	
517	517	7.5	K	M1
631	631	4.4	K	E2
660	660	92.1	K,L	E2
734				
685	685	100.0	K,L	E2
808	808	8.8	K	M1
845	845	21.2	K	E1
	887*	2.1		
896	896	6.0		(E2)
	986*	~9	K	M1
	993	~14	K	M1
	1013*	3.0		
	1028	28	K	M1
	1113*			
	1184*	1.4		
	1199	1.3		
	1231*	3.4		
	1280	3.8		
	1362	1.0		
	1439*	1.2		
	1457	1.3		
	1539	1.6		
	1581*	0.9		
	1801*	0.8		
	1869*	0.5		
	2028*	1.5		
	2199	0.5		
	2486*	0.9		
	2636*	2.4		

NOTE 1: For γ rays above 1028 keV the transition intensity is set equal to photon intensity.

NOTE 2: Asterisk after energy value in column 2 means γ-ray not placed in decay scheme.

^{208}At evaporated on gold-coated Mylar film (0.25 mg/cm^2 thick) was placed in the spectrometer. Electron and γ-spectra were measured simultaneously and the areas under the γ-photopeaks and the corresponding electron peaks were determined and corrected with the appropriate efficiency factors. A typical electron spectrum is shown in fig. 4. To eliminate the possibility that low energy gamma rays might be detected in the silicon counter and be mistaken for electron lines, additional measurements were made with a teflon absorber of sufficient thickness to stop electrons. Measurements were made at 1 to 2 hour intervals to be certain that all electron and photo lines had a 1.7 hour half life.

Measured K, L, and M conversion coefficients are presented in table 2 together with multipolarities deduced by comparison with the theoretical conversion coefficients of Sliv and Band[8]).

In the case of the 177-keV transition the K-conversion electron groups fell between the K_α and K_β X rays and it was possible to get only an order of magnitude value. The "teflon-absorbed" spectrum was helpful in this case. The α_K value of ~0.13 and α_L value of 0.31 rules out all multipolarities except E2.

Table 2

Transition (keV)	Conversion Coefficient	Sliv and Band Values E1	M1	E2	M2	Favored multipolarity
177	$\alpha K = <0.13$ $\alpha L = 0.31$ $\alpha M = 0.12$	.091 0.0165	1.81 0.335	.210 0.42	7.92	E2
206	$\alpha K \simeq 0.9$ $\alpha L = 0.19$ $\alpha M = 0.14$	.0672 .0011	1.20 .22	.165 .22	5.52	M1
517	$\alpha K = 0.062$	.0082	.098	.021	.27	M1 + E2
631	$\alpha K = 0.020$	.0058	.066	.025	.18	E2
660	$\alpha K = 0.0125$ $\alpha L = 0.0043$	.0048	.051	.0125	.16	E2
685	$\alpha K = 0.012$ $\alpha L = \sim 0.004$	.0046	.046	.0118	.14	E2
808	$\alpha K = 0.024$	.0033	.028	.0086	.076	M1
845	$\alpha K = <0.0037$	.0031	.026	.0080	.070	(E1)
896	$\alpha K \approx 0.01$	.0028	.022	.0072	.056	(E2)
986	$\alpha K = 0.012$	.0024	.017	.0059	.042	M1
993	$\alpha K = 0.015$					M1
1028	$\alpha K = 0.017$	.00218	.0161	.00561	.038	M1

2.4. GAMMA-GAMMA COINCIDENCE MEASUREMENTS IN ASTATINE-208 DECAY

Coincidence measurements of conventional type were taken with two germanium detectors of approximately 5 cc sensitive volume. In some experiments the 30 cc germanium crystal was used as one of the detectors. The electronics circuitry consisted of duplicate Goulding-Landis fast-slow coincidence systems[9]. In one system single channel windows were set around the photopeak position of one of the prominent γ rays and the output pulses were used to gate the electronic system associated with the second detector. The resolving time of the fast coincidence network was set at a nominal value of 40 nanoseconds. Measurements were taken with the gating determined by K X rays and by 177, 205, 660, and 685 keV photopeaks.

Results of the experiments are shown in figs. 5 and 6 and summarized in table 3. The most important result is that the prominent γ rays of 177, 660, and 685 keV are in coincidence. Because of the high intensity of these gamma rays it can be concluded that this triple cascade is involved in the majority of decay events; direct decay to the ground or first few excited states is improbable because of the high spin of the parent isotope. The coincidence results alone did not reveal the order of the γ rays in the triple cascade but this information was obtained from the experiments discussed in section 2.5. One of the important omissions from the list of coincident γ rays is the 1028 keV gamma ray (28% abundant in singles spectrum) which is definitely <u>not</u> in coincidence with the 177-keV γ ray and apparently not in coincidence with the 660 and 685-keV γ rays. However, it does appear to be in coincidence with K X rays.

Table 3. Summary of γ γ coincidence results.

Gate Setting	γ rays in coincidence
685	177, 206, 660, 845, 896, 986 + 993
660	177, 206, 685, 845, 986 + 993
177	206, 517, 660, 685, 845, 986, 993
206	177, 660, 685, 845, 993
K-X rays	177, 660, 685, others, 1028

2.5. IN-BEAM MEASUREMENT OF ^{208}Po PROMPT γ RAYS IN ^{209}Bi(p,2n)^{208}Po ^{208}Pb(α,4n)^{208}Po, AND ^{206}Pb(α,2n)^{208}Po REACTIONS

The low-lying levels of ^{208}Po were also studied by observing γ rays in the ^{209}Bi(p,2n)^{208}Po, ^{208}Pb(α,4n)^{208}Po and ^{206}Pb(α,2n)^{208}Po reactions. This in-beam work was done at the Berkeley 88-inch cyclotron by placing a Ge(Li) detector close to the target. Details of these experiments will be published elsewhere[10]).

Figure 7 displays spectra from the ^{209}Bi(p,2n)^{208}Po reaction taken at proton energies of 12, 14, and 16 MeV. A few γ rays belonging to ^{209}Po, a product of the (p,n) reaction, are identified, but most of the γ rays belong to ^{208}Po and in most cases are the same ones seen in the ^{208}At studies. The ^{208}Po radiations observed in these experiments are listed in table 1. The most important information contained in fig. 7 is the shifts in relative intensities of the γ rays when the proton bombarding energy is raised. These shifts are useful for determining the order of placement of the γ rays in the ^{208}Po level scheme, particularly the order of the 684-660-177 keV cascade; the results unambiguously place the 684-keV transition lowest and the 177-keV transition highest. The steady decrease in the intensity difference for these three γ rays is caused by the increasing population of high excited and higher spin states, as discussed by Sakai, Yamazaki, and Ejiri[11]). Figure 7 provides some valuable clues also on the placement of other γ rays in the decay scheme. For example, the 896-keV γ ray appears at a lower energy than the 845-keV γ ray — a fact we make use of in the later discussion.

Similar measurements of ^{208}Po γ rays were made for the ^{208}Po(α,4n)^{208}Po reaction induced by 50-MeV helium ions and the ^{206}Pb(α,2n)^{208}Po reaction. In the prompt spectra from the first reaction prominent γ rays were observed at 145 and 147 keV. These do not occur in the γ-spectrum of ^{208}At.

2.6. IN-BEAM MEASUREMENTS OF DELAYED γ-RAYS OF ^{208}Po PRODUCED IN ^{208}Pb(α,4n)^{208}Po AND ^{206}Pb(α,2n)^{208}Po REACTIONS

Evidence for the existence of ^{208}Po levels with lifetimes in the nanosecond range was found by Yamazaki and Ewan[12]). These experiments were made with a Ge(Li) detector recording γ rays emitted by targets of ^{208}Pb and ^{206}Pb bombarded with helium ions. The beam characteristics of the Berkeley 88-inch cyclotron (repetition period is 100 to 160 nsec and time spread of each bunch is approximately 5 nsec) are such that half lives of delayed transitions can be measured in the period between beam bursts. A fast signal from the Ge(Li) detector was used as a starting signal for a time-to-pulse-height converter and the RF signal from the cyclotron (suitably delayed) was used to stop the converter. The energy and time signals were analyzed in a 2-dimensional pulse height analyzer. Details of the method will be published elsewhere[13]).

It was found that the 177, 660, and 684 cascade gamma rays have a prompt component in their time spectra but in addition they all have a delayed component with a half life of 390 ± 90 nanoseconds as shown in fig. 8 which indicates the existence of a delayed γ-transition feeding the triple cascade. The identity of the delayed transition was not clear from the data.

In addition, it was established that a 147-keV γ ray seen in the ^{208}Pb(α,4n)^{208}Po study had a half life of 8 nanoseconds. This transition is not observed in the radioactive decay of ^{208}At. The 177-keV γ ray showed a faster component of about 4 nsec, but no accurate determination of its half life could be made.

2.7. DELAYED COINCIDENCE MEASUREMENTS IN ^{208}At DECAY

The measurements presented in section 2.6 made it desirable to investigate the possible occurrence of delayed transitions in the decay of ^{208}At even though the coincidence experiments reported in section 2.2 had revealed no evidence for them. As a general introduction to this search we decided to use X rays from the electron capture decay as start pulses for a time-to-pulse-height converter and one or more prominent γ rays as the stop pulses. The population of any long-lived state of ^{208}Po, particularly the 390 nanosecond state, should be revealed by a delayed component in the time-to-pulse-height spectrum of the 177-660-684 cascade.

The detectors consisted of 1-1/2 × 1-1/2 inch NaI(Tl) crystals cemented to 56 AVP photomultiplier tubes. The fast anode signals were fed into 100 Mc tunnel diode discriminators, the outputs of which fed into an EG & G Time-to-Amplitude Converter (TAC). The energy signals from the preamplifiers were fed into conventional electronic circuitry using single channel analyzers to set appropriate gates. The gated output of the TAC was fed into a 400 channel pulse height analyzer. The time resolution of this system (FWHM) was 2 nanoseconds at the energies measured. The TAC was gated on by the polonium X rays emitted by the ^{208}At sample and off by the 177-keV γ ray. The time spectrum so obtained is shown in fig. 9. The presence of a 380 nanosecond component in this time spectrum proves that some unidentified level lying above the 177-660-684 cascade is being populated at least partially by ^{208}At decay. In section 2.9 we discuss an experiment which leads to the conclusion that in fact approximately 35 percent of the decay events pass through this delayed level.

In a second experiment in which a shorter time range was emphasized we observed a shorter component of 4.0 ± 0.5 nanoseconds. The results of this experiment are shown in fig. 10. We believe this period belongs to the 177-keV transition. It is only in rough agreement with the value predicted for E2 by the Weisskopf formula but is orders of magnitude larger than the value predicted for E1.

2.8. ANGULAR DISTRIBUTION OF γ RAYS IN 177-660-684 CASCADE

The angular distribution of the prominent 177, 660, 684 KeV γ rays was measured in the in-beam experiments to obtain additional evidence for the assignments of multipolarities and level spins.

The experiment was done with the $^{208}Pb(\alpha,4n)^{208}Po$ reaction, where the target nucleus has no spin and, moreover, the lead metal used as the target has cubic crystal structure. Also in this set of experiments the time analysis system was used so that we could measure the angular distribution of delayed γ rays as well as prompt γ rays. Since the half life of the delayed state (380 nsec) is much greater than the repetition period of the beam burst (127 nsec) we took the integrated delayed component that did not include the prompt component. The results computed from measurements made at 90, 112, 134, and 156 degrees are presented in table 4. The angular distribution of the delayed component is found to be the same ($A_2 \sim 0.12$, $A_4 \sim -0.03$) within the errors for all three transitions. This result is compatible only with the sequence[15],

$$6+ \xrightarrow{E2} 4+ \xrightarrow{E2} 2+ \xrightarrow{E2} 0+ \quad ,$$

Table 4. Angular distribution of γ rays in $^{208}Pb(\alpha,4n)^{208}Po$ reaction at E_α = 48 MeV. Metallic foil of ^{208}Pb was used as a target.

γ ray energy (keV)	Prompt		Delayed	
	A_2	A_4	A_2	A_4
177	0.161 ± 0.018	-0.080 ± 0.026	0.134 ± 0.015	-0.043 ± 0.022
660	0.149 ± 0.032	-0.008 ± 0.049	0.128 ± 0.038	-0.019 ± 0.054
685	0.116 ± 0.031	-0.057 ± 0.048	0.100 ± 0.035	-0.015 ± 0.055
206	-0.273 ± 0.024	-0.090 ± 0.036		

although the absolute values of A_2 are about 50% lower than the empirically expected ones[16]). The angular distributions of the prompt components show a well-known tendency, toward a decrease in anisotropy for the transitions lower in the sequence. The study of the angular distribution of delayed γ rays from the viewpoints of the hyperfine interaction will be reported elsewhere by Yamazaki and Matthias[17]).

The 206-keV γ rays exhibited angular distribution characteristic to the $J+1 \rightarrow J$ dipole transition. The measured L conversion coefficient rules out E1 (see table 2) and is in reasonable agreement with M1. Consideration of both experiments establishes an M1 multipolarity.

2.9. ESTIMATION OF POPULATION OF 380 nsec STATE OF ^{208}Po IN DECAY OF ^{208}At

Evidence for the participation of a 380 nanosecond ^{208}Po level in the decay scheme of ^{208}At is presented in section 2.7. In earlier sections evidence was presented for the occurrence of a 177-660-684 keV cascade to the ground state in the great majority of decay events. (In our final decay scheme we conclude that 79% of the events pass through this triple cascade.) These facts made it possible to estimate the fraction of decay events passing through the 380 nanosecond state by the following method.

First we determined the singles spectrum of an ^{208}At sample and computed the ratio of polonium K_α X rays to photopeaks of the 660-keV and 684-keV γ rays. Then under nearly identical conditions we measured the spectrum of K_α X rays plus 660 and 684-keV photons in prompt coincidence with 177-keV photons. This was done with two Ge(Li) detectors in the manner outlined in section 2.4. If for the moment we attribute all the K X rays to the orbital electron capture process and ignore any contribution from γ-conversion, we can conclude that any reduction in the $K_\alpha/660\gamma$ or $K_\alpha/684\gamma$ ratio

in the coincidence spectrum compared to the singles spectrum must be caused by the population of the 380 nanosecond level; when the delayed state is populated the X ray is removed from the coincidence spectrum but the 660 and 684-keV photons remain. From this rough computation we estimated that about 40 percent of the ^{208}At decay events populate the 380 nanosecond level.

It is of course necessary to correct the X ray intensity in singles and coincidence spectra for contributions from K-conversion of several γ rays. We carried out a detailed calculation correcting for these effects for counter efficiencies, fluorescent yield, etc. and obtained the corrected value of 35 percent for the events which pass through the 380 nanosecond level. The algebra is straightforward but too lengthy to reproduce here.

3. Level Scheme of ^{208}Po

3.1. CONSTRUCTION OF LEVEL SCHEME

The experimental information presented in the preceding sections can be used to construct the level scheme for ^{208}Po shown in fig. 11. In the paragraphs which follow we discuss the proposed scheme level-by-level together with the evidence used in support of each.

685 keV level. This is the first excited state of ^{208}Po. The 685-keV transition, which is the most intense γ ray in the spectrum, is a member of the promient 685-660-177 triple cascade of γ rays (main sequence), and the reaction data clearly place it at the bottom of the sequence. Both angular distribution and conversion coefficient experiments characterize it as E2, which establishes the 685-keV state as 2+, the expected value for the first excited state of an

even-even nucleus. Intensity balance precludes direct population of this level. Furthermore, it is nearly certain that the spin of ^{208}At is >4 (see later discussion) so no decay to the 685-keV level would be expected.

1345 keV level. The second most intense line in the γ spectrum is the 660-keV γ. It is in cascade with the 177 and 685 keV transitions, and the (p,2n) work (fig. 7) clearly places it between them. Angular distribution and conversion coefficient values argue that it is J+2 $\rightarrow$ J E2. This evidence together with the absence of a 1345-keV γ ray establishes that the 1345-keV level is 4+. From an intensity balance of the γ rays in the spectrum, we conclude there is no direct population of this level by electron capture.

1419 keV level. A 734 keV γ-ray is observed in the ^{209}Bi(p,2n) reaction spectra displayed in fig. 7. It appears to have built up to its full intensity at a proton energy of 14 MeV, which indicates that it originates from a state near the 1522 keV level and distinctly below the 2200 keV region. Because of the wide spacing of the first two ^{208}Po levels the 734 keV radiation must originate from a level at 1419 keV. This γ ray is not observed in ^{208}At decay.

1522 keV level. The third principal line in the spectrum is the 177-keV transition. It is of nearly equal intensity with the other two members of the main sequence and is in coincidence with them. The (p,2n) work (fig. 7) shows that it is the highest lying of the three, and its E2 nature is established by conversion coefficient and by angular distribution measurements. The E2 nature of the 177-keV γ ray and the interpretation of the angular distribution measurements presented in section 2.8 establishes a 6+ assignment for the 1522-keV level. The level has a half life of 4.0 nsec. From the in-out balance of γ-transitions electron-capture branching to this level cannot exceed 2 percent.

1581 keV level. The 896-keV γ ray present in 7% intensity is not coincident with the 177 nor the 660-keV transitions, but is coincident with the 685-keV radiation (figs. 5 and 6). The (p,2n) reaction data in fig. 7 indicate that the 896-keV γ ray originates from a state near the 1522-keV level and definitely below the 2200-keV region. Owing to the wide spacing of the first two ^{208}Po levels, the 896-keV transition can originate only from a level at 1581 keV. From our estimate of the K conversion coefficient, the 896-keV radiation is most likely E2. There is a weak γ-line at 1581 keV (0.9%) which could possibly be the crossover transition to the ground state but we have no strong evidence for this placement. The most probable spin and parity of the 1581 keV level is 4+. As direct electron capture to a 4+ level is impossible from a 7+ ground state of ^{208}At (discussed later) there must be some γ transitions totaling about 6% feeding this level. However we have not been able to identify these γ rays and none are shown in fig. 11.

2153 keV level. A level at 2153-keV can be postulated to account for the 631- and 808-keV γ rays which differ in energy by 177 keV. The 631-keV radiation is in coincidence with the 177-keV transition, but the 808-keV radiation is not. The coincidence data (fig. 5) for γ-radiation coincident with 660- or 685-keV photons are not good enough in the neighborhood of 808-keV to establish the coincidence of the 808-keV γ ray with 660-and 685-keV transitions. However, the (p,2n) reaction (fig. 7) data show that both the 631-and 808-keV γ's originate at some level above 1511 keV, and below 2300 keV. Conversion coefficients for both of these lines have been measured, leading to the multipolarity assignments listed in table 2. This would establish the 2153-keV level as 5+ or 6+. Intensity balance argues that this level must be largely populated by a direct electron-capture branch.

2367 keV level. One of the more prominent peaks in the spectrum is at 845 keV, (21%). This γ ray is strongly coincident with the 177-keV line, and the rest of the main sequence. The (p,2n) reaction curves show that it originates from a level considerably above 1522 keV. The intensity of the 845-keV peak, the clear coincidence data, and the absence of any other coincident γ's of proper energy or intensity all argue that the 845-keV transition feeds directly into the 1522-keV level, which establishes a level at 2367 keV. We could only obtain an upper limit of 3.7×10^{-3} for the conversion coefficient of the 845-keV line, but this low value clearly indicates that it is E1 (see table 2). The 2367-keV level is therefore 5-, 6-, or 7-. There is, however, no γ ray of 1023 keV, which would correspond to the transition to the 1345-keV 4+ level via another E1 γ ray. The 2367-keV level is therefore 6- or 7-. Considering the high intensity of the 845-keV line, and the low intensities of the γ's which feed the level (fig. 11), we can estimate that about 20% of ^{208}At electron capture decays feed directly into the 2367-keV level.

2515 keV level. This level is postulated principally on the basis of the moderately intense (14%) 993-keV transition which is strongly coincident with the 177-keV line, and the rest of the main sequence. The (p,2n) reaction curves indicate that this γ ray originates from a level higher than 2400 keV, but the strength of the coincidence with the 177-keV line, and the absence of other coincident γ's of comparable intensity argue that the 993-keV γ ray feeds directly into the 1522-keV level. This establishes, then, a level at 2515 keV. The 206-keV transition is coincident with the 993-keV line, but it is also coincident with the 845-keV γ, and it is of insufficient intensity to be fed by both of these gammas. It must therefore feed into them, and the absence of any other low energy gamma rays argues that the 206-keV transition feeds directly

into the 2515 keV level. This would require a 148-keV branch to the 2367-keV level. Such a peak is observed, particularly in the highest bombarding energy spectrum of the (p,2n) work (fig. 7). A weak peak at this energy is also seen in the ^{208}At γ-spectra. The 993-keV conversion coefficient has been measured (table 2), and corresponds to an M1 character, giving possible assignments of 5, 6, 7+ to the 2515 keV level. The absence of an 1170-keV peak in the spectrum which would correspond to an M1 transition from the 2515 to the 1345-keV level is inconsistent with a 5+ assignment for the 2515 keV level, leaving 6+ or 7+ as the favored choice.

2721 keV level. Reasons were given above in connection with the 2515-keV level for believing that the 206-keV γ-transition (12% intensity) terminates at that level. This would then establish a level at 2721 keV. A peak at 1199 keV appears in the spectrum (1.3% intensity), which should correspond to the transition from the 2721 to the 1522-keV level. Angular distribution results (see section 2.8) prove that the 206 keV γ is $J+1 \rightarrow J$ M1. On the basis of this multipolarity the spin and parity choices for the 2721-keV level are restricted to 6, 7, 8+. The absence of a 1376 keV γ ray of E2 character feeding the 4+ level at 1345-keV is inconsistent with a 6+ assignment, leaving 7+ or 8+ as the remaining possibilities.

2802 keV level. The 1457 keV (1.3%) and 1280 (3.8%) keV gamma rays differ in energy by 177 keV, and can be used to postulate a level at 2802 keV. The intensities of these high energy transitions were such that no coincidence data could be obtained to verify this placement. This level, decaying as it does to the 6+ and 4+ levels at 1522 and 1345 keV respectively, may be 5+, 6+, or 5-. This level is almost certainly fed by direct electron capture branching.

2884 keV level. The highest level in the scheme is found at this energy. It is deexcited by transitions of 2199, 1539, 1362, and 517 keV to the levels at 685, 1345, 1522, and 2367 keV respectively. The intensity balance indicates a 10% population of this level by electron capture.

3.2. PLACEMENT OF THE 380 NANOSECOND STATE

The placement of the prominent 1028 keV transition and the assignment of the 380 nanosecond state to a level lying near 1532 keV is based on the following considerations.

The transition lifetime measurements discussed in sections 2.6 and 2.7 prove that the delayed state feeds directly or indirectly into the top of the main triple γ cascade and hence must lie above 1522 keV. Furthermore, the experiments discussed in section 2.9 establish a value of 35 percent for the fraction of the total events which pass through the 380 nanosecond state, which means that the transition (or series of transitions) connecting the delayed state with the 1522-keV level should be prominent both in the singles spectra and in the γ spectra coincident with photons of 177, 660, and 685 keV. Also the radiation should have an apparent decay component of 380 nanoseconds in the spectra taken between beam bursts in the $^{206}Pb(\alpha,2n)$ and $^{208}Pb(\alpha,4n)$ reaction studies. Because no such properties were observed for any of the γ rays listed in table 1, we can conclude that a transition of low energy was being overlooked. From our experimental γ spectra we can state that we should not have missed photons of the required intensity with an energy 10 keV or above. Of course, if the transition energy were this low it would be almost totally converted unless it were E1 in character. In our electron spectra (not all shown here) we did not observe electrons of the missing transition down to 20 keV.

It is probable that the 1028-keV γ ray plays a major role in the population of the 380 nanosecond state. For one thing, it occurs in 28 percent abundance which is roughly equal to the 35 percent intensity of the 380 nanosecond state. It is in coincidence with K-x rays which shows that it does not originate in a level of long life, but it is not in coincidence with any other γ ray which indicates that it populates a state with a long lifetime. The other possible conclusion, that the 1028 keV gamma ray decays directly to ground, is ruled out by the fact that it was not observed in the ^{209}Bi(p,2n) reaction studies.

A further arguement can be made on the basis of the intensity figures. If the 380 nanosecond level is populated by paths quite independent of the level responsible for the 1028 keV gamma ray, then 35 + 28 = 63 percent of the decay events of ^{208}At pass through one or the other of these levels, leaving only 37 percent for the population of the remaining states. But in the previous discussion we have accounted for more than 50 percent of the total intensity in the population of levels which are quite unrelated to the 380 nanosecond state or the 1028 keV radiation. Hence we are foreced to conclude that the 1028 keV γ ray feeds into the 380 nanosecond state.

Our placement of the 380 nanosecond state in fig. 11 can be considered reasonable by a comparison of the similar scheme in ^{210}Po. Theory in this case (see for example the work of Kim and Rasmussen[18])), predicts a 0+, 2+, 4+, 6+, 8+ sequence for the lowest lying levels formed from the $h^2_{9/2}$ proton configuration. The 0+ state is greatly depressed and the spacing in the 2+ to 8+ sequence becomes successively smaller. The position of these levels up to the 6+ is well known experimentally from the decay scheme of ^{210}At[19]). The work of Yamazaki and Ewan[12]), on delayed radiation observed in the

$^{208}Pb(\alpha,2n)^{210}Po$ case provides evidence for an 8+ state with a half life of 150 nanoseconds, although the 8+ → 6+ γ ray was not observed directly. It is quite reasonable to expect a similar set of levels in ^{208}Po and the 380 nanosecond state could be the 8+ level in the corresponding sequence. If this is correct, the missing γ ray transition is E2 in character. A half life of 380 nanoseconds is quite reasonable for an E2 transition of less than 20 keV. We discuss this interesting 8+ → 6+ transition more fully in the discussion section below.

3.3. ELECTRON CAPTURE BRANCH AND LOG FT VALUES

The Q value for the electron capture decay of ^{208}At to ^{208}Po is estimated to be 4823 keV by Myers and Swiatecki[20]. Almost the same value is given also in other tables[21-23]. Assuming this value and the correctness of the present decay scheme, we deduced log ft values, as presented in table 5 and in fig. 11.

4. Discussion

4.1. ^{208}At GROUND STATE AND LOG FT VALUES

The ground state spin-parity of ^{208}At can be predicted from the simple shell-model. The single-proton orbits at Z=83 and the single-neutron orbits at N=125[24]) are presented in fig. 12. The ground state of ^{208}At (Z=85, N=123) should then have the unpaired configuration, $(h_{9/2})_p\ (f_{5/2}^{-1})_n$, which results in the ground-state spin of 7+ according to the Nordheim rule[25]).

This prediction is quite consistent with the observed log ft values, although we cannot exclude other cases. For instance, the ^{208}At ground state

Table 5. Electron capture branches and ft values. Q_{EC} = 4823 keV is assumed.

Level		Ec	
Energy (keV)	Spin-parity	Branch (%)	log ft
0	0+	0	
685	2+	0	
1345	4+	< 2	> 8.0
1522	6+	< 2	> 8.2
~1532	8+	7	7.4
1581	(4+)	6	7.5
2153	(5+)	13	7.0
2367	6-,7-	12	7.0
2515	6+,7+	~2	~7.7
~2560	7+,8+	28	6.6
2721	7+,8+	15	6.8
2802	5+,6+,5-	5	7.2
2884		10	6.9

decays to both 6+ and 8+ states. The fairly high log ft values seem to be reasonable, since the transition

$$(h_{9/2}{}^{3})_p\ (f_{5/2}{}^{-1})_n\ ,\ 7^+ \rightarrow (h_{9/2}{}^{2})_p,\ 6^+ \text{ or } 8^+$$

is forbidden because of $\Delta\ell = 2$. Forbiddenness of this type has been observed[19] in the decay of ^{210}At to ^{210}Po, where the transition

$$(h_{9/2}{}^{3})_p\ (p_{1/2}{}^{-1})_n\ ,\ 5^+ \rightarrow (h_{9/2}{}^{2})_p\ ,\ 4^+ \text{ or } 6^+$$

is much more hindered because $\Delta\ell = 4$.

4.2. ^{208}Po STRUCTURE IN COMPARISON WITH ^{206}Pb AND ^{210}Po

The excited states of ^{208}Po can be described qualitatively in terms of those of ^{206}Pb and ^{210}Po. The level schemes of ^{206}Pb and ^{210}Po have been studied mainly from the decays of ^{206}Bi[24] and ^{210}At[19], respectively, which populate levels with spins between 4 and 7. In fig. 13 are presented those levels to be compared with ^{208}Po. A large number of configurations can contribute to the many levels in the spin range 0-7 observed in these complex level schemes. Therefore it seems meaningless without a detailed theoretical calculation to attempt a one to one correspondence between more than a few levels of these nuclei. Level assignments on the basis of the weak coupling approximation can be most safely made to the low-lying levels of higher spin, because the number of configurations contributing to such levels is very limited.

The recent experiment of Yamazaki and Ewan[12]) on the $^{208}Pb(\alpha,2n)^{210}Po$ reaction has revealed the 8+ member of the $h_{9/2}^{2}$ configuration in ^{210}Po, as shown in fig. 13. This is an isomeric state of 150-nsec half life. Because of the absence of 6+ and 8+ levels in ^{206}Pb at this energy region, we expect the 6+ and 8+ states of the $h_{9/2}^{2}$ configuration of protons to remain nearly unperturbed in ^{208}Po. Our 380-nsec isomeric state at about 1542 keV must be the 8+ member of the $(h_{9/2}^{2})_p$ configuration. The 4 nsec 6+ state at 1522 keV in ^{208}Po also corresponds to the 6+ state in ^{210}Po quite well, as indicated by the dotted line in fig. 13. The correspondence of the 1345-keV 4+ state in ^{208}Po to the 1426-keV 4+ state in ^{210}Po is fair, but not as good as for the 6+ and 8+ states. The reason for this is the presence of a 4+ level at 1684 keV in ^{206}Pb, which gives rise to configuration mixing for the 4+ state of ^{208}Po. The first 2+ state at 685 keV in ^{208}Po must involve contributions from proton and neutron excitations. On the other hand, the 3+ level of ^{208}Po may be the almost pure neutron state appearing in ^{206}Pb.

4.3. STRUCTURE OF THE $h_{9/2}^{2}$ BAND

We have characterized the lowest 4+, 6+ and 8+ levels in ^{208}Po as members of the $(h_{9/2}^{2})_p$ band. As is discussed by Yamazaki[26]), experimental B(E2) values in the $h_{9/2}^{2}$ band of ^{210}Po are well described in terms of $e_{eff} = 1.6$, which is also consistent with the static quadrupole moment of ^{209}Bi. In table 6 are presented experimental B(E2) values in ^{210}Po and ^{208}Po computed under the assumption of the theoretical conversion coefficients of Sliv and Band[8]). The $8+ \rightarrow 6+$ transition energy of ^{210}Po is unknown, but assumed to be 35 keV in the derivation of B(E2). However, we can still obtain a reasonable value of B(E2) because the energy dependence of half life for

such a low energy E2 transition is quite small. This is true because the total conversion coefficient has an approximate energy dependence of E^{-5} in the energy range of interest.

The B(E2, $6^+ \rightarrow 4^+$) for ^{208}Po is twice the corresponding B(E2, $6^+ \rightarrow 4^+$) for ^{210}Po. This fact suggests that configuration mixing in ^{208}Po is responsible for the enhancement of the $8^+ \rightarrow 6^+$ E2 transition. On the other hand, the situation for the $8^+ \rightarrow 6^+$ transitions is suprising. The half life of the 8^+ state in ^{208}Po is considerably greater than that of the 8^+ state in ^{210}Po which suggests an extremely low transition energy or a smaller B(E2) in ^{208}Po. For instance, if the $8^+ \rightarrow 6^+$ transition energy is assumed to be 20 keV the B(E2) becomes 29 e^2fm^4, which is a factor of 2 smaller than the corresponding B(E2) in ^{210}Po. We will attempt a weak coupling treatment[28] of the $h_{9/2}^2$ members in a vibrating ^{206}Pb core to see what level structure and B(E2) can be anticipated.

To the lowest order of surface coupling, the perturbed states become

$$
\begin{aligned}
|I^+\rangle = {} & a_1^I |(h_{9/2}^2) I \ , \ (0\,\hbar\omega)0 \ ; \ I\rangle \\
& + a_2^I |(h_{9/2}^2) I\text{-}2 \ , \ (1\,\hbar\omega)2 \ ; \ I\rangle \\
& + a_3^I |(h_{9/2}^2) I \ , \ (1\,\hbar\omega)2 \ ; \ I\rangle \\
& + a_4^I |(h_{9/2}^2) I\text{+}2 \ , \ (1\,\hbar\omega)2 \ ; \ I\rangle
\end{aligned}
$$

The energies E_I and the mixing amplitudes a_i^I can be obtained by diagonalizing the interaction[28]

$$H_{int} = -k \sqrt{\frac{\hbar\omega}{2C}} \sum_{\mu} \left| b_{\mu} + (-)^{\mu} b_{-\mu}^{\dagger} \right| \left| Y_{2\mu}(\theta_1,\phi_1) + Y_{2\mu}(\theta_2,\phi_2) \right| \quad ,$$

where k is the coupling constant which has a magnitude of 40 MeV according to Bohr and Mottelson[29]. However we leave k as a parameter. The vibrational amplitude is given by

$$\sqrt{\frac{\hbar\omega}{2C}} = \frac{\sqrt{B(E2,\ 2^+ \rightarrow 0^+,\ ^{206}Pb)}}{\frac{3}{4\pi} ZeR_o^2} = 0.0146 \quad ,$$

evaluated with the experimental value[24]

$$B(E2,\ 2^+ \rightarrow 0^+,\ ^{206}Pb) = 214\ e^2fm^4 \quad .$$

The non-diagonal matrix elements are

$$\langle (j^2)J,\ NR;\ IM|H_{int}|(j^2)J',\ N'R';\ IM\rangle$$

$$= -2k \sqrt{\frac{\hbar\omega}{2C}} \langle NR\|b + b^{\dagger}\|N'R'\rangle \langle j\|Y_2\|j\rangle$$

$$\times \sqrt{(2J+1)(2J'+1)}\ W(jJjJ';\ j2)\ W(JRJ'R';\ I2)$$

The E2 transition matrix element is

$$\langle I-2\|\mathcal{M}(E2)\|I\rangle = a_1^{I-2}\ a_1^{I} \langle (j^2)I-2\| \sum_{p=1,2} e_{eff}\ r_p^2 Y_{2\mu}(\theta_p,\phi_p)\|(j^2)I\rangle$$

$$+ \left(\sqrt{\frac{2I+1}{5}}\ a_1^{I-2}\ a_2^{I} + \sqrt{\frac{2I-3}{5}}\ a_1^{I}\ a_4^{I-2} \right) \langle 0\| \frac{3}{4\pi} ZeR_o^2\ \overset{\circ}{\alpha}_2\|\hbar\omega\rangle$$

and then

$$B(E2,\ I \rightarrow I-2) = \frac{1}{2I+1} \left|\langle I-2 \| \mathcal{M}(E2) \| I \rangle\right|^2$$

$$= \Big| a_1^{I-2}\, a_1^{I} \sqrt{B(E2,\ I \rightarrow I-2,\ ^{210}Po)} - \left(a_1^{I-2}\, a_2^{I} + \sqrt{\frac{2I-3}{2I+1}}\, a_1^{I}\, a_4^{I-2}\right) \times \sqrt{B(E2,\ 2^+ \rightarrow 0^+,\ ^{206}Pb)} \Big|^2$$

Since a_2^{I} and a_4^{I-2} are negative, the contribution of the surface vibration is always additive.

Calculated energy levels and B(E2) are illustrated in fig. 14. This simple calculation has yielded the following results. The $6^+ \rightarrow 4^+$ level spacing increases as k, while the $8^+ \rightarrow 6^+$ level spacing decreases rapidly as k and the level order is ultimately changed. Because of the uncertainty of E_8 at $k \rightarrow 0$ we cannot make a quantitative statement on the spacings but the trends seem to explain our experimental results quite well. Thus we are led to believe that the longer half life of the 8^+ state in ^{208}Po is due to the small level spacing as expected from this calculation. The calculated $6^+ \rightarrow 4^+$ energy spacing is smaller than experimental value of 177 keV, which implies that the 4^+ state involves more configuration mixing than considered here. The calculated B(E2) value increases with k, but it is smaller than the experimental $B(E2,\ 6^+ \rightarrow 4^+)$ for ^{208}Po. This also suggests that the present treatment is too simple to take into account configuration mixing for the 4^+ state.

More realistic calculations including proton-neutron interaction[30] would explain the whole level structure, but it is beyond scope of the present paper.

Table 6. B(E2) in the $h_{9/2}^2$ band.

Nucleus	Transition	Transition energy	Half life (nsec)	B(E2) (e^2fm^4)
^{210}Po	8+ → 6+	(35)[a]	150[b]	50
	6+ → 4+	46.5	38[c]	245
^{208}Po	8+ → 6+		380[b,d]	
	6+ → 4+	177	4.0[d]	450

a) Assumed
b) From ref. 12)
c) From ref. 28)
d) Present data

4. Concluding Remarks

We believe this study has established a number of features of the low lying levels of ^{208}Po and suggested a basis for their interpretation. We believe it also serves as a good demonstration of the advantages of a simultaneous study of a given isotope by the traditional decay scheme approach and the newer techniques of on-line reaction spectroscopy. We hope our results can serve as a solid starting point for further experimental and theoretical studies of this interesting nucleus.

Acknowledgements

We should like to acknowledge the contributions of Drs. G. T. Ewan, E. Matthias, and S. G. Prussin to the experimental work done at the 88 inch cyclotron. We owe thanks to Dr. M. Redlich for helpful discussions on the 8+ isomeric level and to Dr. K. Harada for advice on the calculations. One of us (TY) acknowledges the support of the Miller Institute of the University of California and expresses his thanks to Professor I. Perlman and J. O. Rasmussen for hospitality in permittinghim the use of the facilities of the Nuclear Chemistry Division of the Lawrence Radiation Laboratory. He also owes thanks to Dr. J. M. Hollander for encouragement and support. Finally we are as usual indebted to the crews of the 88-inch cyclotron and the Heavy Ion Linear Accelerator.

Footnotes and References

*This work was performed under the auspices of the U.S. Atomic Energy Commission.

†Present address: U. S. Naval Radiological Defense Laboratory, San Francisco, California.

‡Present address: Department of Physics, University of Tokyo.

1) E. K. Hyde, A. Ghiorso, G. T. Seaborg, Phys. Rev. 77 (1950) 765

2) G. W. Barton, A. Ghiorso, and I. Perlman, Phys. Rev. 82 (1951) 13

3) P. E. Thoresen, F. Asaro, and I. Perlman, J. Inorg. Nucl. Chem. 26 (1964) 1341

4) A. W. Stoner, Ph.D. thesis, University of California, June 1956, University of California Radiation Laboratory Report UCRL-3471, June 1956.

5) E. K. Hyde, J. Am. Chem. Soc. 74 (1952) 4181 and Report NAS-NS-3003 "The Radiochemistry of Francium". Available from Office of Technical Services, Dept. of Commerce, Washington 25, D. C.

6) E. Elad and M. Nakamura, Nucl. Instr. Methods 37 (1965) 327 and 42 (1966) 315

7) H. T. Easterday, A. J. Haverfield, and J. M. Hollander, Nucl. Instr. Methods 32 (1965) 333. See also, Haverfield, Ph.D. thesis University of California Lawrence Radiation Laboratory Report UCRL-16969, November 1966

8) Tables of Internal Conversion Coefficients, L. A. Sliv and I. M. Band, Appendix 5 in Vol. 2 of $\alpha\beta\gamma$ Spectroscopy, ed. Kai Siegbahn, North Holland Publishing Company, Amsterdam, 1965

9) F. Goulding and D. Landis, Linear Amplifier, Gating and Timing System, in Instrumentation Techniques in Nuclear Pulse Analysis, NRC-NAS Publication 1181

10) T. Yamazaki, unpublished results, 1967

11) M. Sakai, T. Yamazaki and H. Ejiri, Nucl. Phys. 74 (1965) 81

12) T. Yamazaki and G. T. Ewan, Phys. Letters 24B (1967) 278

13) T. Yamazaki and G. T. Ewan, Nucl. Instr. Methods, to be published

14) For half life estimates based on Weisskopf's relationship we used the nomograms given in Wapstra, Nijgh, and Van Lieshout, Nuclear Spectroscopy Tables, North Holland Publishing Company, Amsterdam, 1959, Ch. 6

15) See, for instance, T. Yamazaki, University of California Lawrence Radiation Laboratory Report UCRL-17086, September 1966; Nuclear Data, Section A, 3 (1967) 1

16) R. M. Diamond, E. Matthias, J. O. Newton and F. S. Stephens, Phys. Rev. Letters 16 (1966) 1205

17) T. Yamazaki and E. Matthias, to be published

18) Y. E. Kim and J. O. Rasmussen, Nucl. Phys. 47 (1963) 184

19) See the most recent work: S. G. Prussin and J. M. Hollander, University of California Lawrence Radiation Laboratory Report UCRL-17843 (September 1967); submitted for publication in Nuclear Physics

20) W. D. Myers and W. J. Swiatecki, University of California Lawrence Radiation Laboratory Report UCRL-11980 (May 1965); Nucl. Phys. 81 (1966) 1

21) J. H. E. Mattauch, W. Thiele and A. H. Wapstra, Nucl. Phys. 67 (1965) 1, 32, 73

22) M. Yamada and Z. Matsumoto, J. Phys. Soc. JAPAN 16 (1961) 1497

23) V. E. Viola, Jr. and G. T. Seaborg, J. Inorg. Nucl. Chem. 28 (1966) 697

24) See C. M. Lederer, J. M. Hollander and I. Perlman, "Table of Isotopes, sixth ed" (Wiley, New York, 1967)

25) See, for instance, M. G. Mayer and J. H. D. Jensen, "Elementary Theory of Nuclear Shell Structure" (Wiley, New York, 1955)

26) T. Yamazaki, to be published in the Proceeding of the 1967 Enrico Fermi International School of Physics at Varenna (Academic Press)

27) See for instance, D. C. Choudhury, Mat. Fys. Medd. Dan. V.d-Selsk. 28 (1954) no. 6; G. Alaga and G. Ialongo, Phys. Letters 22 (1966) 619

28) E. G. Funk, Jr., H. J. Prask, F. Schima, J. McNulty and J. W. Mihelich, Phys. Rev. 129 (1962) 757

29) A. Bohr and B. R. Mottelson, Mat-Fys. Medd. Dan V.D-Selsk 27 (1953) no. 16

30) For the case of ^{212}Po, see N. K. Glendenning and K. Harada, Nucl. Phys. 72 (1965) 481

Figure Captions

Fig. 1. Gamma spectrum from pure ^{208}At sample. All spectra taken with 2 × 3 cm × 8 mm Ge(Li) detectors. Upper curve is 50 minute count taken 3 hours after HILAC bombardment. Second and third curves represent same counting period starting 7 hours and 11 hours respectively after bombardment.

Fig. 2. Gamma spectrum from pure ^{208}At sample. Spectrum measured with 30 cc coaxial Ge(Li) detector. Time 30 minutes. Energy scale calibrated with many standards including radiations of ^{54}Mn, ^{22}Na, ^{137}Cs, ^{207}Bi, and ^{228}Th series.

Fig. 3. Photons emitted by ^{208}At in the X ray region as measured by high resolution photon spectrometer. Astatine-208 prepared by extraction in diisopropyl ketone from pure ^{212}Fr solution. Spectrum shows $L_\alpha L_\beta L_\gamma$ and $K_{\alpha_2} K_{\alpha_1} K_{\beta_1}$ and K_{β_2} X rays of polonium. Fluorescent X rays of several elements were used to calibrate energy scale. Note that no radiations other than polonium X rays are observed in this energy region.

Fig. 4. Electron spectrum of ^{208}At sample measured by silicon semiconductor detector in conversion coefficient spectrometer. Time of measurement 66 minutes.

Fig. 5. Results of $\gamma\,\gamma$ coincidence measurements of ^{208}At radiations with 2 Ge(Li) detectors of ~5 cm^3 sensitive volume. Time for each measurement — 4 hours. Upper curve shows γ rays in coincidence with 660-keV γ ray. Lower curve shows γ rays in coincidence with 685-keV γ ray.

Fig. 6. Results of γ γ coincidence measurement of ^{208}At radiations made with Ge(Li) detectors of ~5 cm^3 and 30 cm^3 sensitive volume. Smaller crystal used to select gate pulses corresponding to 177-keV γ ray. Only those sections of spectrum where coincidence peaks appeared are shown. For comparison a singles spectrum is shown above. A slight time base shift occurred in the two measurements. The occurrence of a 177-keV peak in the coincidence spectrum is the spurious result of Compton photons from the prominent 660 and 685-keV γ rays falling in the gate channels.

Fig. 7. Prompt γ rays recorded with 5 cm^3 Ge(Li) detector in in-beam measurements of ^{209}Bi(p,2n)^{208}Po at 3 proton beam energies.

Fig. 8. Time distribution curves for prominent γ rays emitted by ^{208}Po in the interval between beam bursts in the reaction ^{206}Pb(α,2n)^{208}Po. Start pulses for the pulse-height circuitry were supplied by the γ-detector and stop pulses came from a delayed signal taken from the cyclotron RF oscillator.

Fig. 9. Time-to-pulse-height spectrum of ^{208}At radiations. Po K X rays used as start pulses, 177-keV γ rays as stop pulses.

Fig. 10. Time-to-pulse-height spectrum of ^{208}At radiations. Polonium X rays used as start pulses and 177-keV photons as stop pulses. Single channel analyzer selection on both radiations indicated is shown in the inset by horizontal bars. The 4 nsec component of the delay curve is assigned to the 177-keV γ ray. Time of measurement — 200 minutes. Prompt curve measured with radiations of ^{22}Na.

Fig. 11. Decay scheme of ^{208}At showing ^{208}Po levels and transitions. The numbers in parentheses are percent transition intensities ($I_\gamma + I_e$). The established coincidence relation is indicated by a circle at the transition arrow. The 1419 keV level appears only in the (p,2n) reaction.

Fig. 12. The single-proton orbits at Z=83 and the single-neutron-hole orbits at N=125, revealed in the energy levels of ^{209}Bi and ^{207}Pb, respectively.

Fig. 13. Comparison of the $^{208}_{84}Po_{124}$ levels with the $^{206}_{82}Pb_{124}$ and $^{210}_{84}Po_{126}$ levels. Levels of similar character are connected by dotted lines. Spin and parity of each level are given to the left and the energies (in keV) to the right.

Fig. 14. Level structure and B(E2) values obtained in the weak coupling calculation as function of the coupling strength k. Because of the large uncertainty in the ground state energy, only relative energies are meaningful.

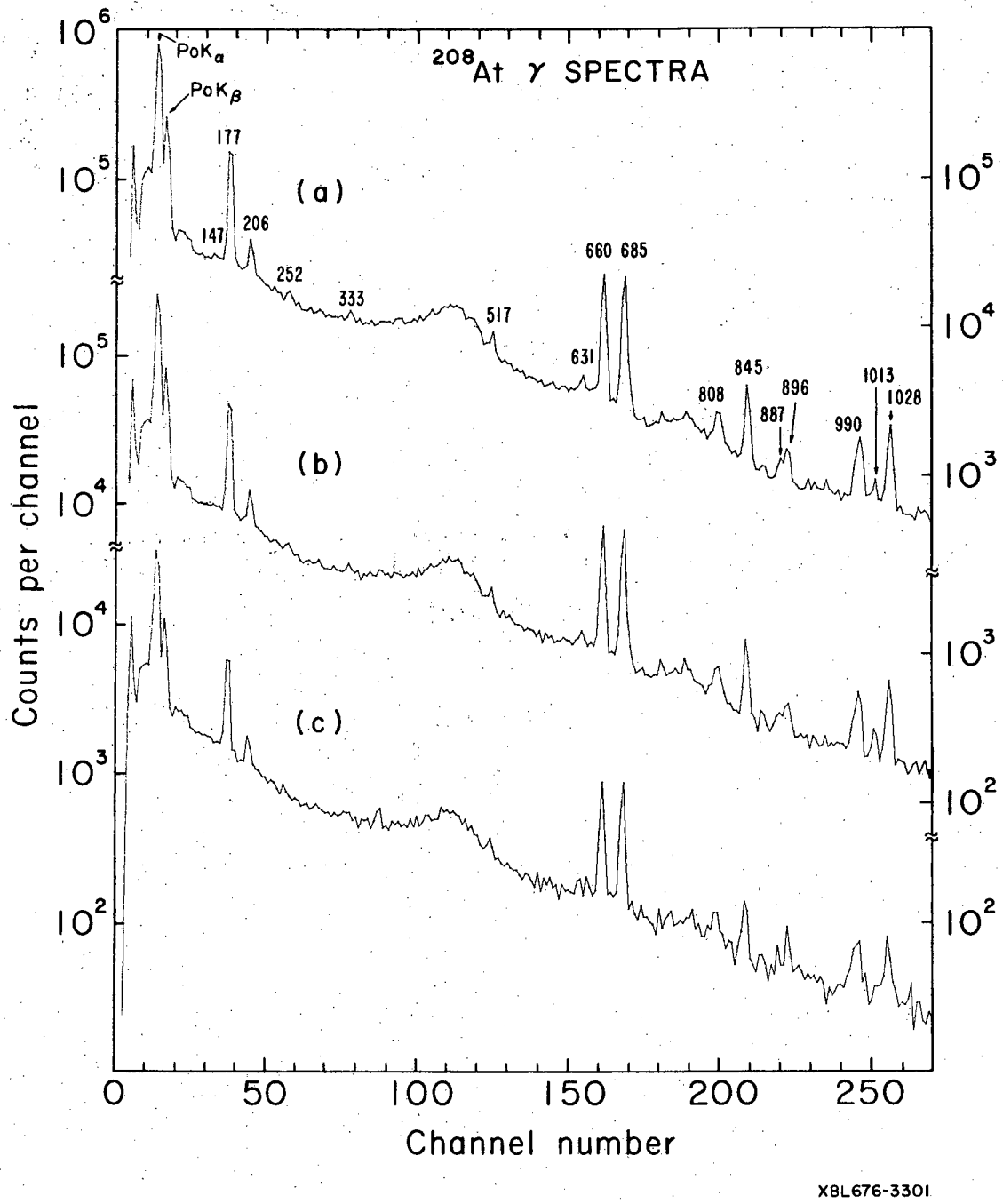
^{208}At γ SPECTRA
PoK$_\alpha$
PoK$_\beta$
177
147
206
252
333
517
631
660 685
808
845
887
896
990
1013
1028
(a)
(b)
(c)
Counts per channel
Channel number
0
50
100
150
200
250
XBL676-3301

Fig. 1

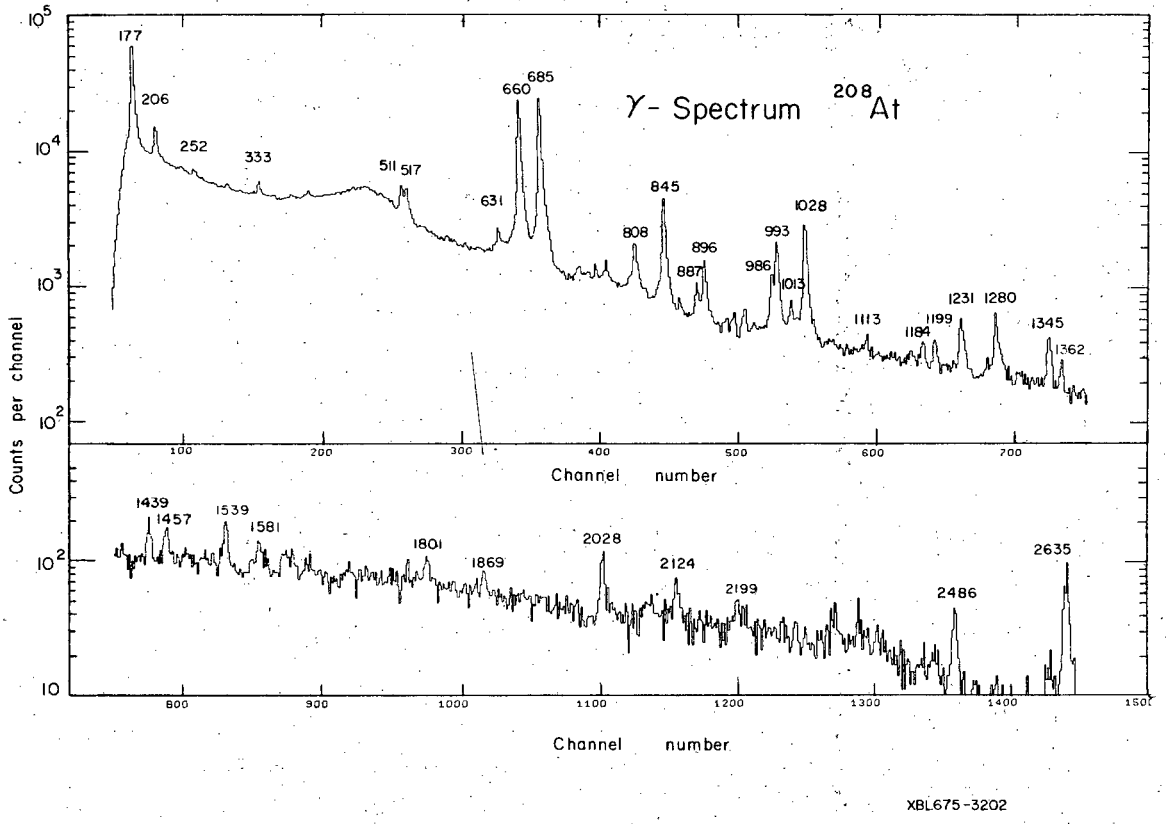
γ- Spectrum 208At
Counts per channel
Channel number
Channel number
177
206
252
333
511
517
631
660
685
808
845
887
896
986
993
1013
1028
1113
1184
1199
1231
1280
1345
1362
1439
1457
1539
1581
1801
1869
2028
2124
2199
2486
2635
XBL675-3202

Fig. 2

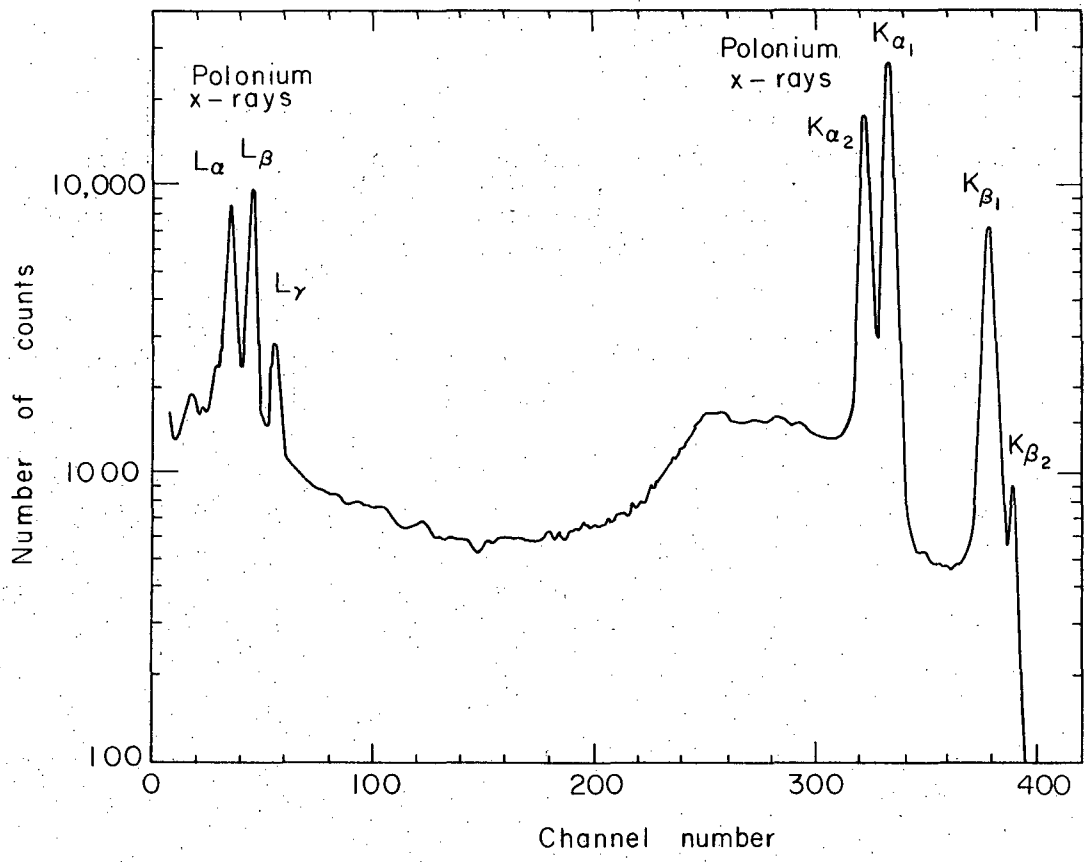

XBL675-3200

Fig. 3

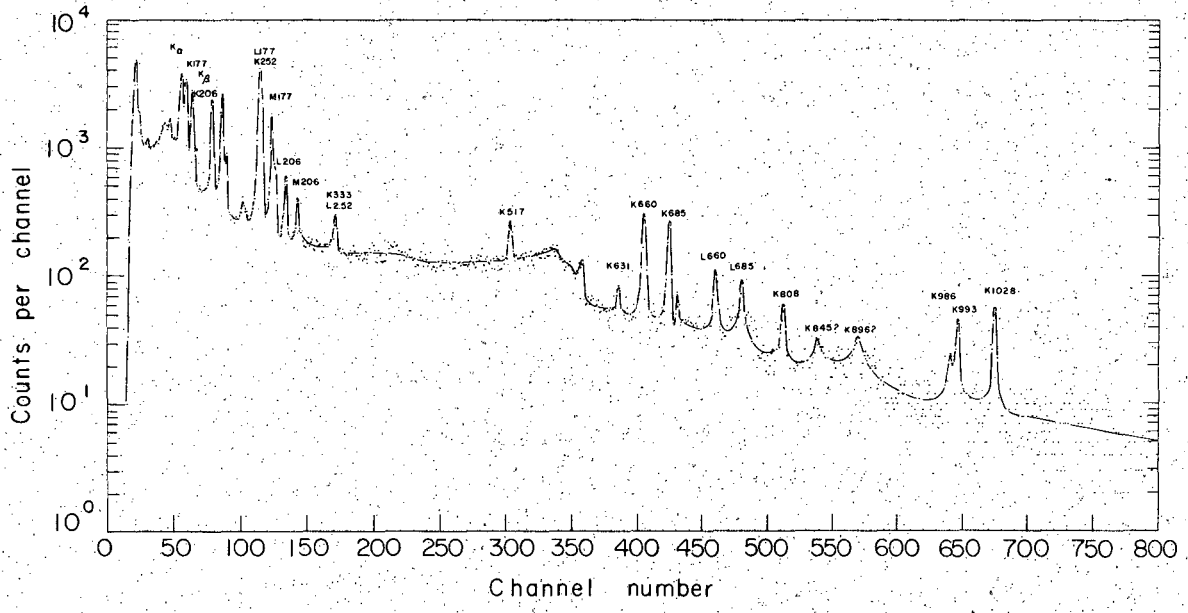

XBL675-3201

Fig. 4

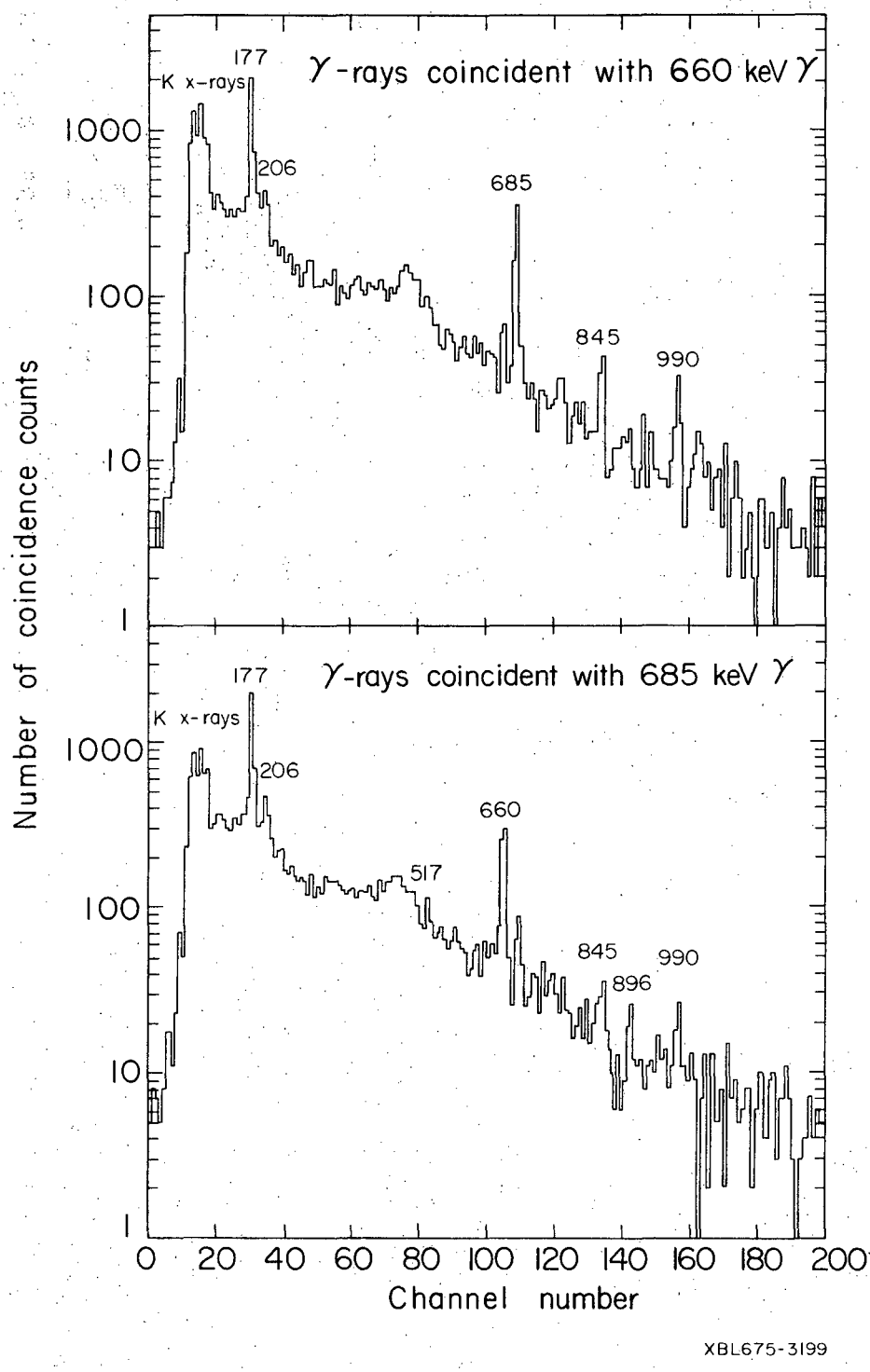
γ-rays coincident with 660 keV γ
K x-rays
177
206
685
845
990
γ-rays coincident with 685 keV γ
K x-rays
177
206
517
660
845
896
990
Number of coincidence counts
1000
100
10
1
0 20 40 60 80 100 120 140 160 180 200
Channel number
XBL675-3199

Fig. 5

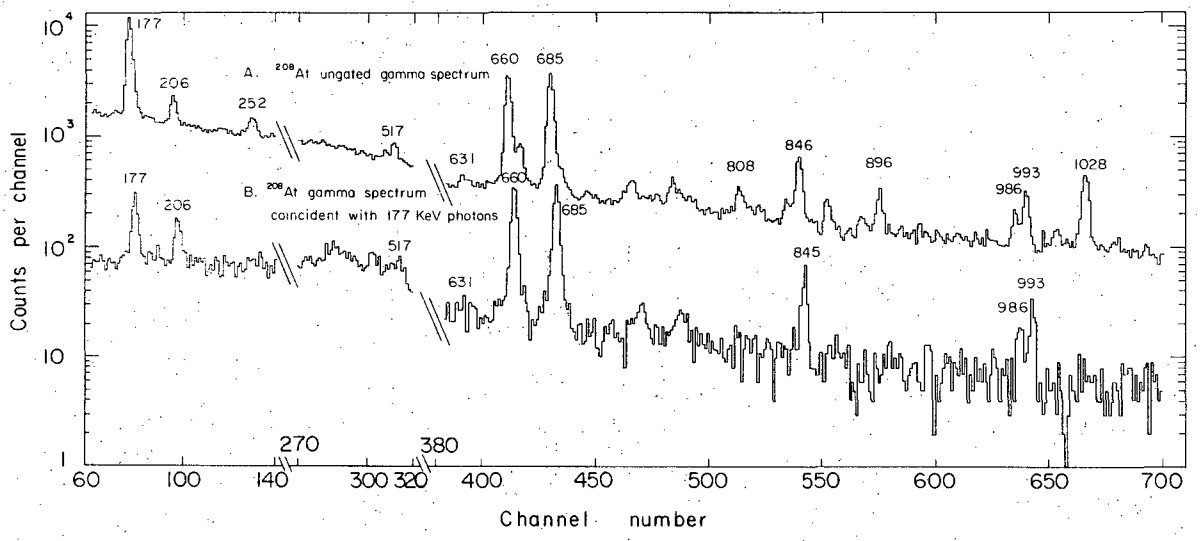
A. ^{208}At ungated gamma spectrum
B. ^{208}At gamma spectrum coincident with 177 KeV photons
Counts per channel
Channel number
177
206
252
517
631
660
685
808
846
896
986
993
1028
845
270
380
XBL675-3198

Fig. 6

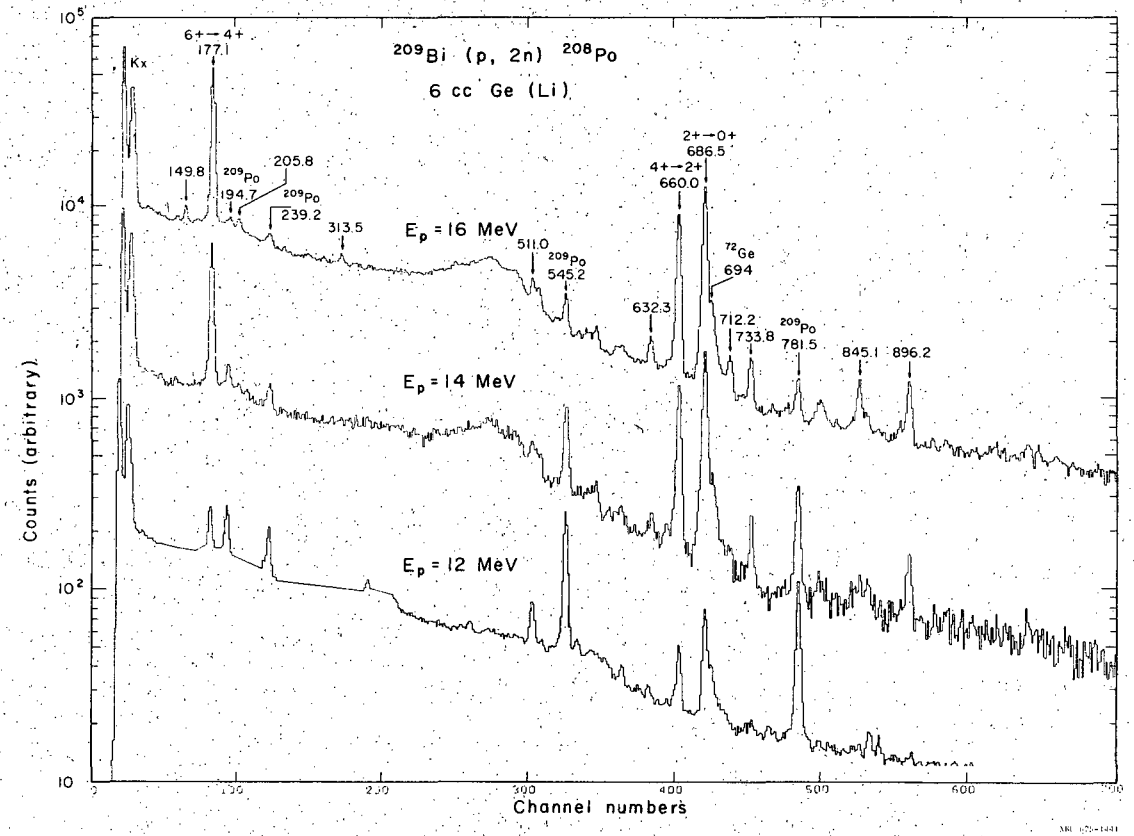
209Bi (p, 2n) 208Po
6 cc Ge (Li)
Kx
6+→4+
177.1
149.8
209Po
205.8
194.7
209Po
239.2
313.5
Ep = 16 MeV
511.0
209Po
545.2
632.3
4+→2+
660.0
2+→0+
686.5
72Ge
694
712.2
733.8
209Po
781.5
845.1
896.2
Ep = 14 MeV
Ep = 12 MeV
Counts (arbitrary)
Channel numbers

Fig. 7

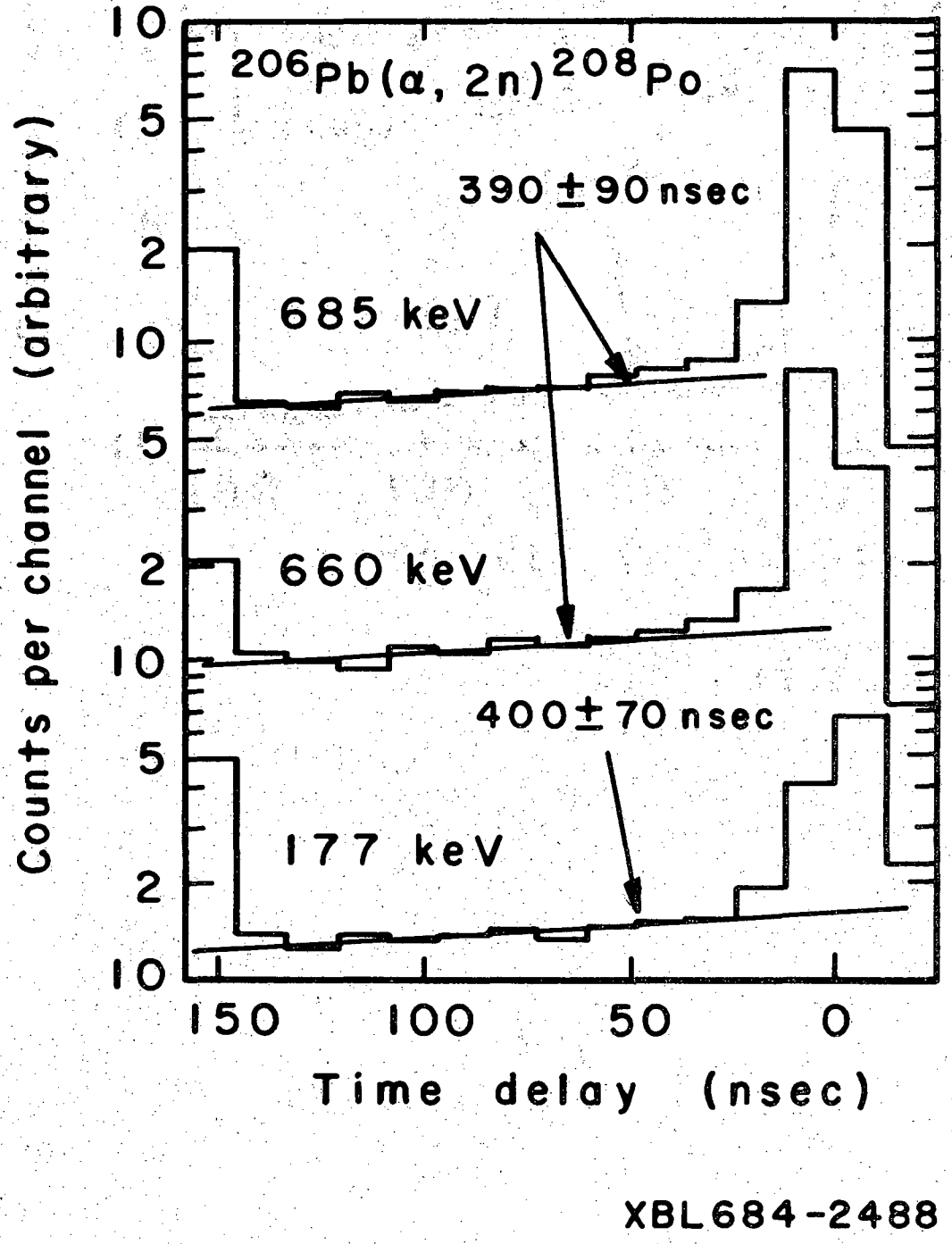
$^{206}Pb(\alpha, 2n)^{208}Po$
390 ± 90 nsec
685 keV
660 keV
400 ± 70 nsec
177 keV
Counts per channel (arbitrary)
Time delay (nsec)
10
5
2
10
5
2
10
5
2
10
150
100
50
0
XBL684-2488

Fig. 8

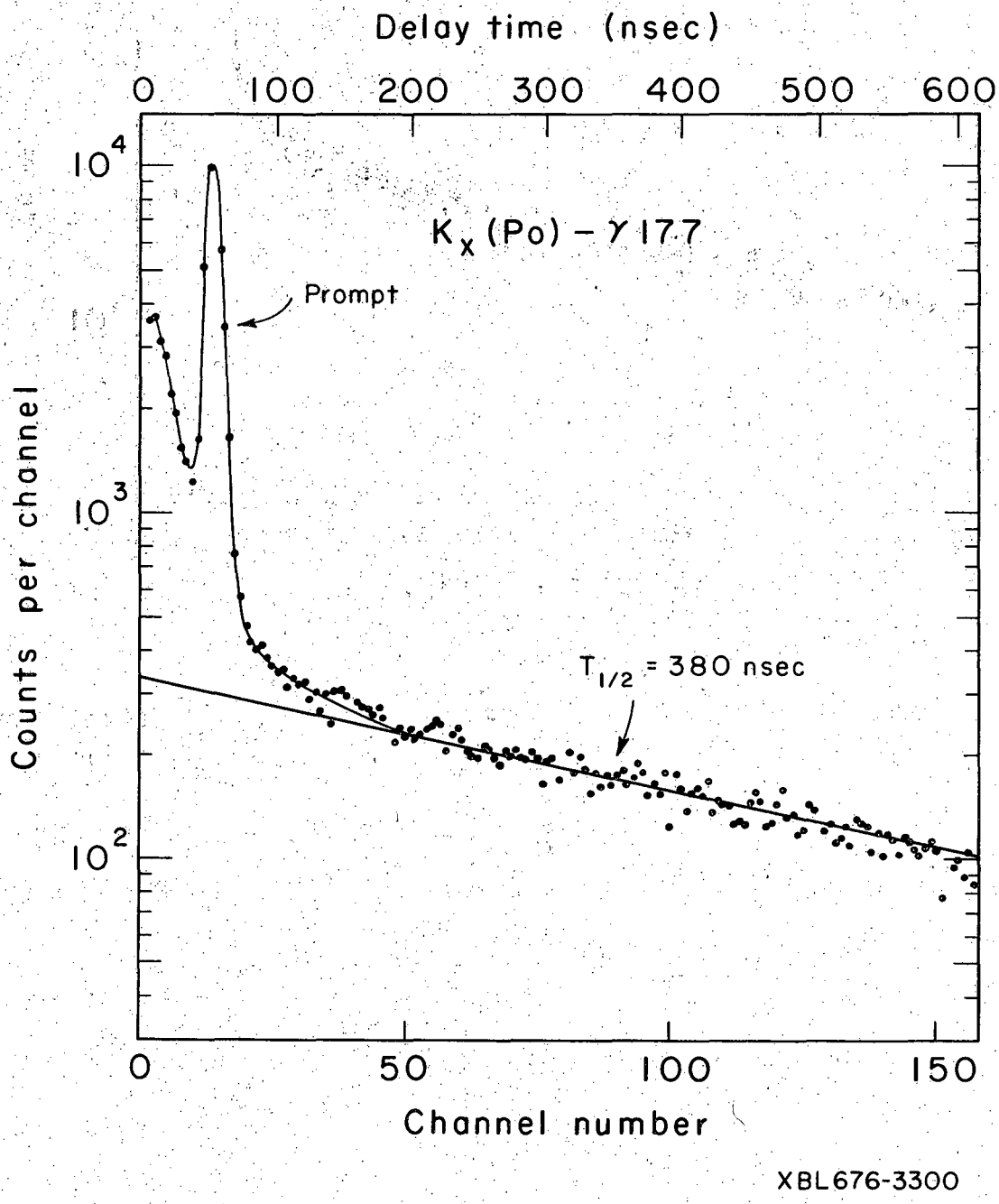
Delay time (nsec)
0
100
200
300
400
500
600
10^4
10^3
10^2
K_x (Po) – γ 177
Prompt
$T_{1/2}$ = 380 nsec
Counts per channel
0
50
100
150
Channel number
XBL676-3300

Fig. 9

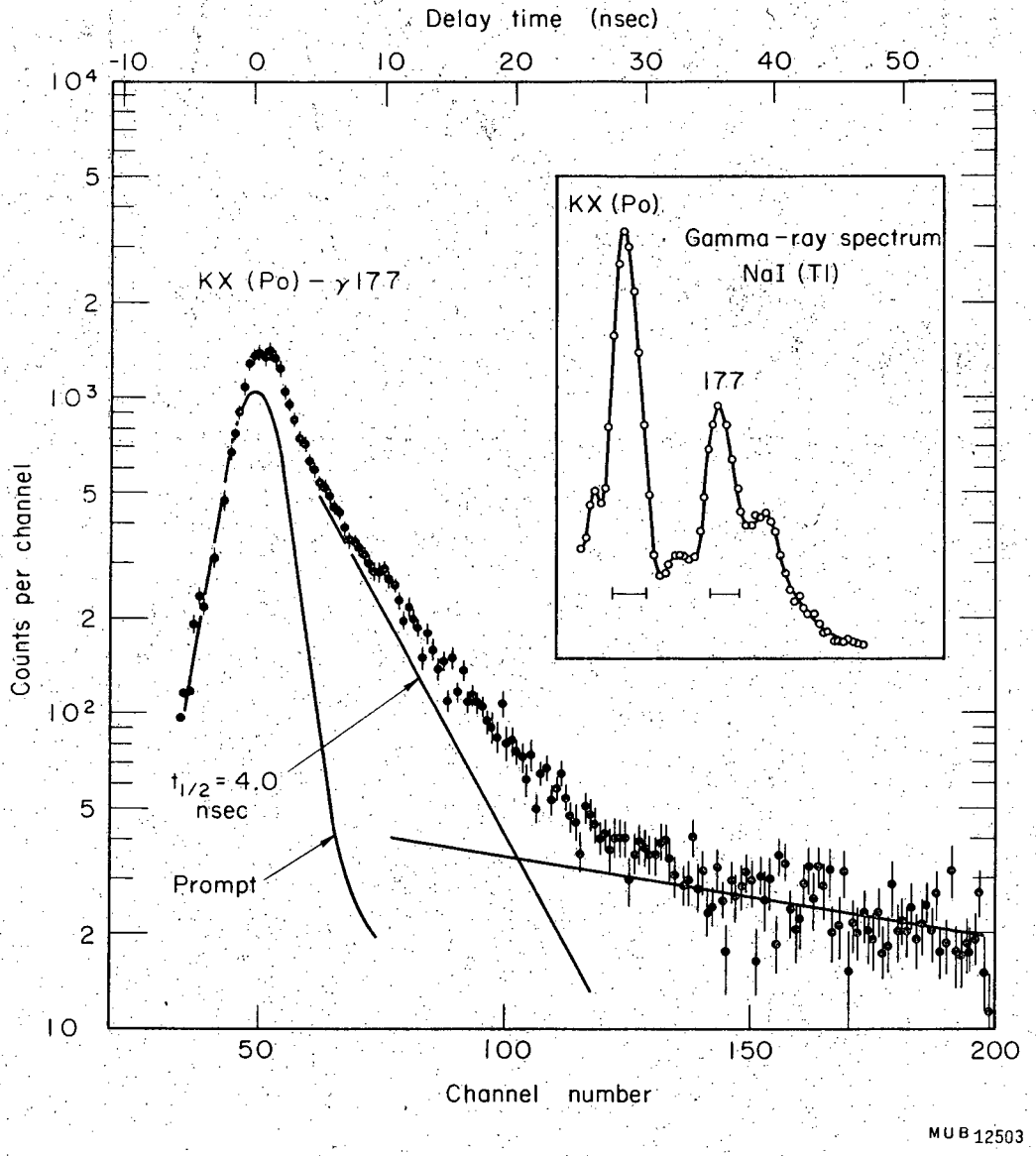
Delay time (nsec)
-10
0
10
20
30
40
50
10^4
5
2
10^3
5
2
10^2
5
2
10
Counts per channel
KX (Po) – γ 177
KX (Po)
Gamma-ray spectrum
NaI (Tl)
177
$t_{1/2}$ = 4.0 nsec
Prompt
50
100
150
200
Channel number
MUB 12503

Fig. 10

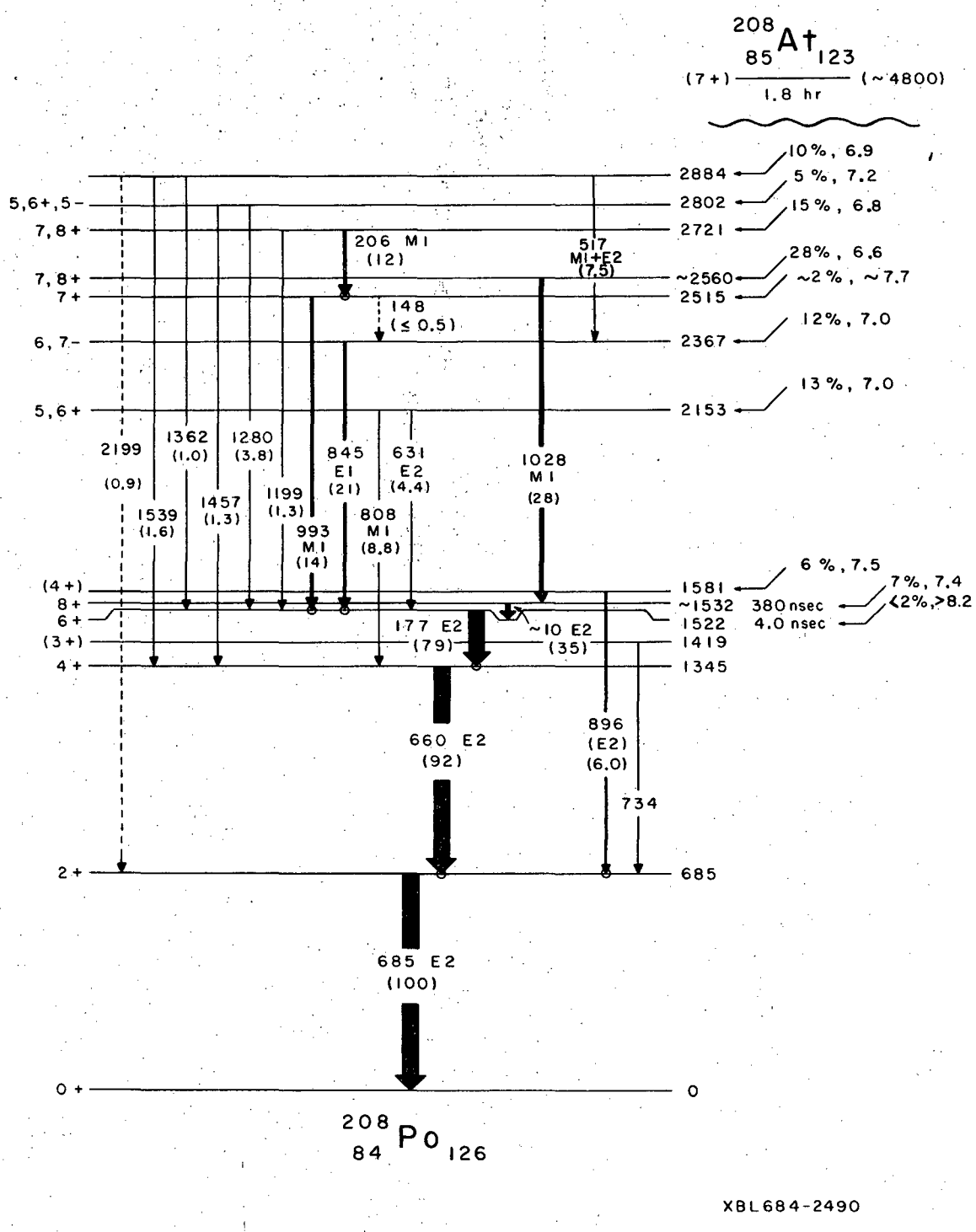
208 85 At 123
(7+)
1.8 hr
(~4800)
10%, 6.9
5%, 7.2
15%, 6.8
28%, 6.6
~2%, ~7.7
12%, 7.0
13%, 7.0
6%, 7.5
7%, 7.4
<2%, >8.2
380 nsec
4.0 nsec
2884
2802
2721
~2560
2515
2367
2153
1581
~1532
1522
1419
1345
685
0
5,6+,5-
7,8+
7,8+
7+
6,7-
5,6+
(4+)
8+
6+
(3+)
4+
2+
0+
206 M1 (12)
517 M1+E2 (7.5)
148 (≤ 0.5)
2199 (0.9)
1362 (1.0)
1280 (3.8)
1539 (1.6)
1457 (1.3)
1199 (1.3)
993 M1 (14)
845 E1 (21)
631 E2 (4.4)
808 M1 (8.8)
1028 M1 (28)
177 E2 (79)
~10 E2 (35)
660 E2 (92)
896 (E2) (6.0)
734
685 E2 (100)
208 84 Po 126
XBL684-2490

Fig. 11

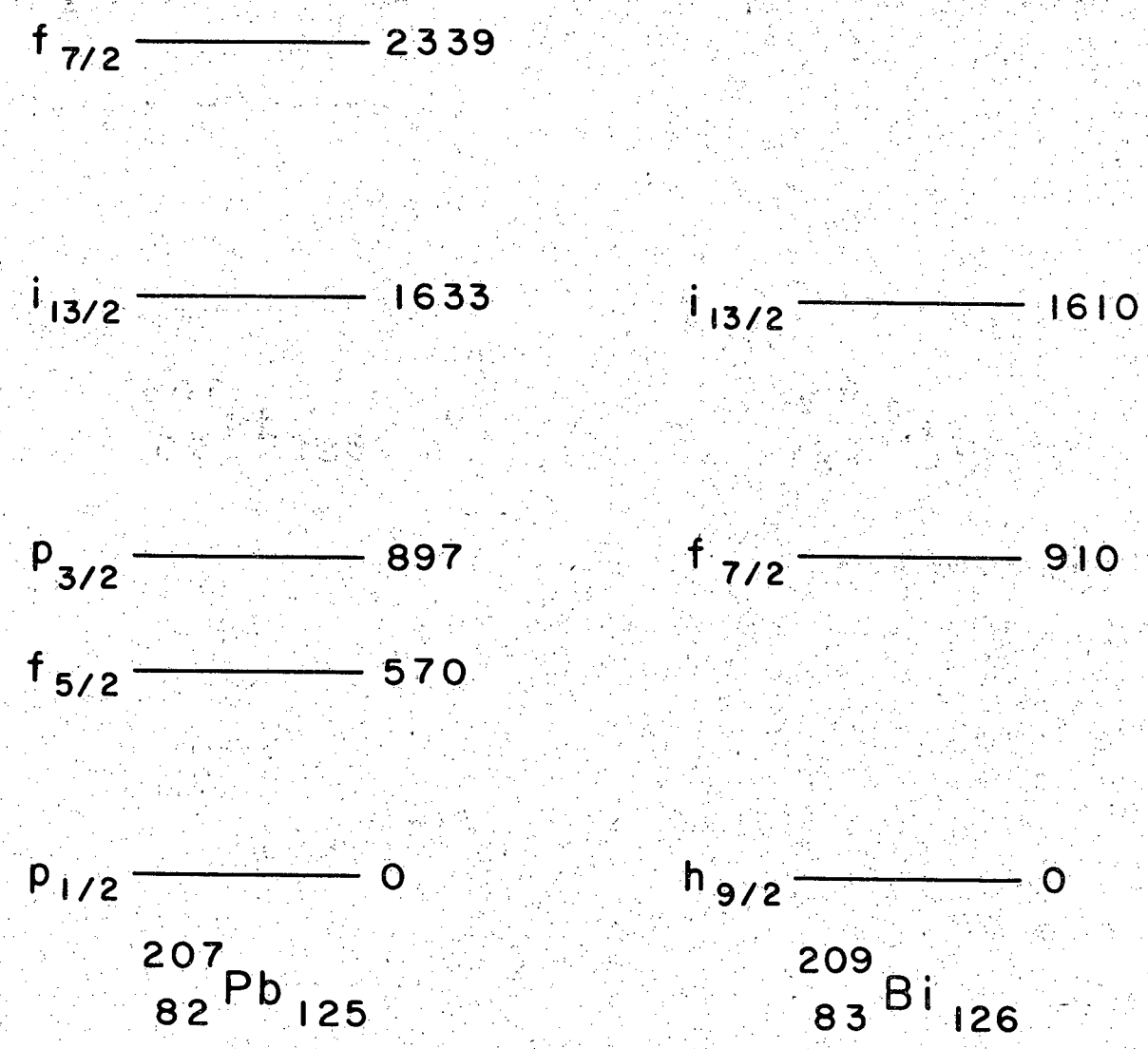
f 7/2
2339
i 13/2
1633
p 3/2
897
f 5/2
570
p 1/2
0
207 82 Pb 125
i 13/2
1610
f 7/2
910
h 9/2
0
209 83 Bi 126
XBL684-2489

Fig. 12

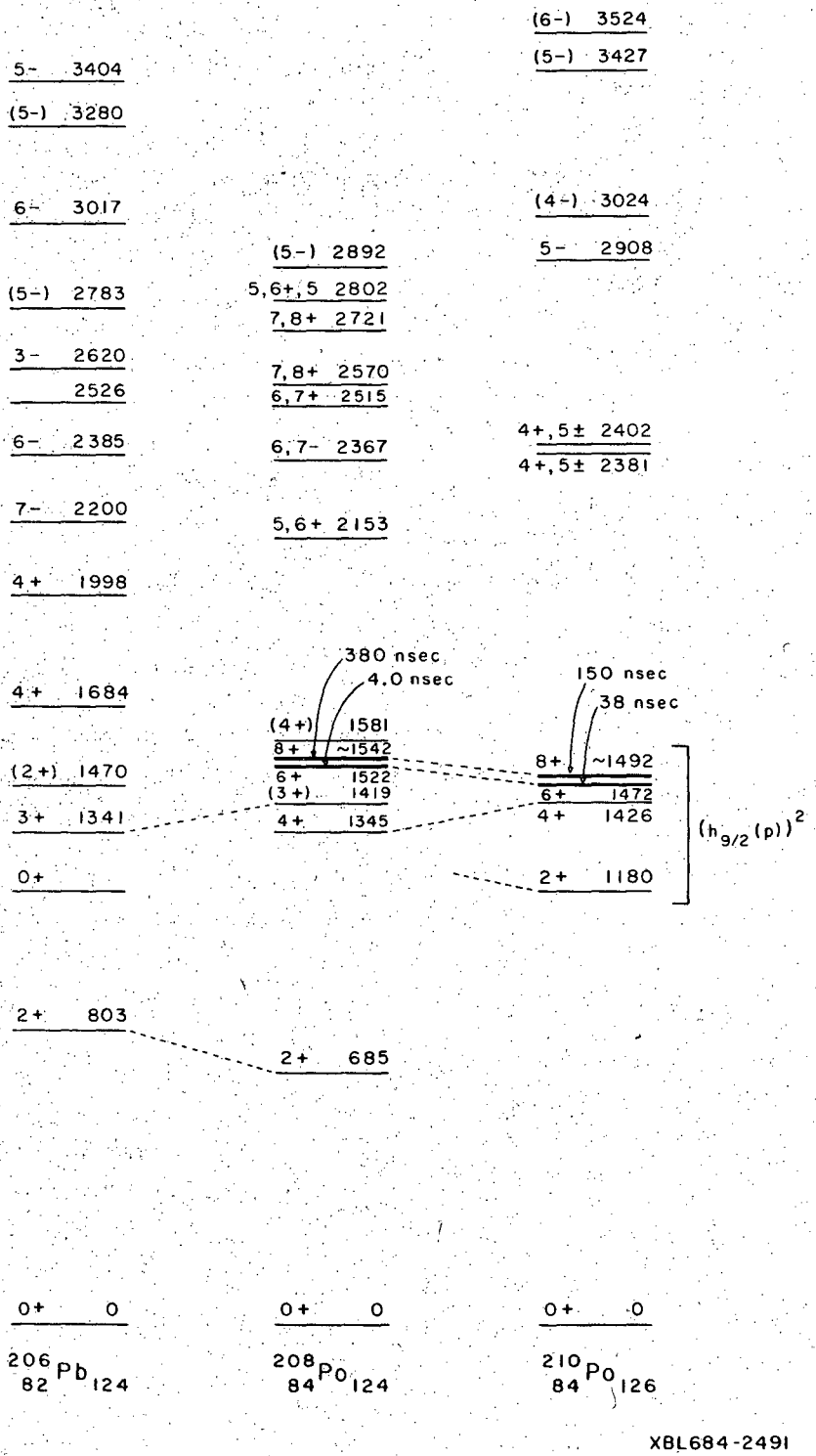
(6-) 3524
(5-) 3427
5- 3404
(5-) 3280
(4-) 3024
6- 3017
5- 2908
(5-) 2892
5,6+,5 2802
(5-) 2783
7,8+ 2721
3- 2620
7,8+ 2570
2526
6,7+ 2515
4+,5± 2402
6- 2385
6,7- 2367
4+,5± 2381
7- 2200
5,6+ 2153
4+ 1998
380 nsec
4.0 nsec
150 nsec
38 nsec
4+ 1684
(4+) 1581
8+ ~1542
8+ ~1492
(2+) 1470
6+ 1522
6+ 1472
(3+) 1419
3+ 1341
4+ 1345
4+ 1426
(h9/2(p))2
0+
2+ 1180
2+ 803
2+ 685
0+ 0
0+ 0
0+ 0
206 82 Pb 124
208 84 Po 124
210 84 Po 126
XBL684-2491

Fig. 13

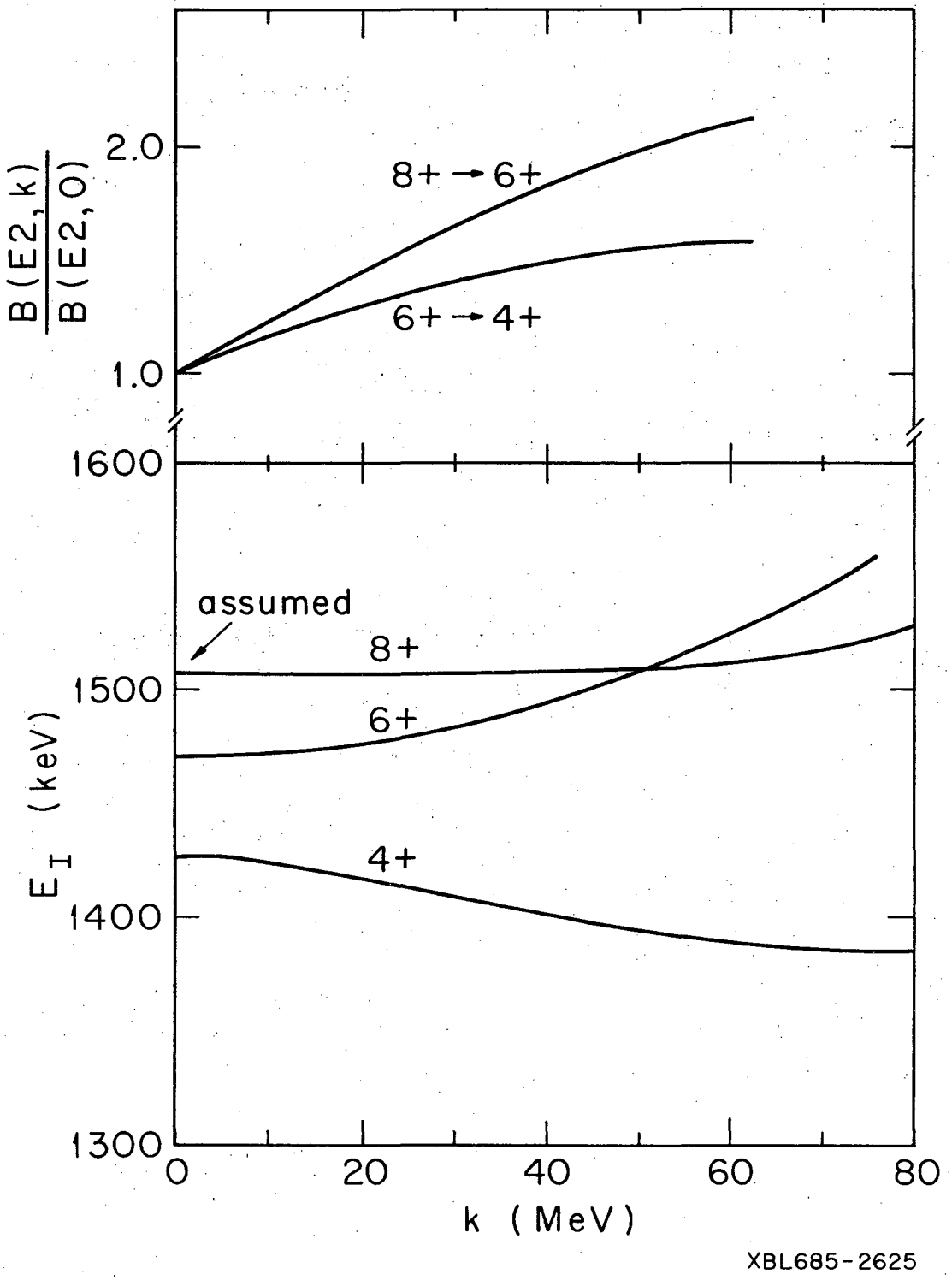
B(E2,k)/B(E2,0)
2.0
1.0
8+ → 6+
6+ → 4+
1600
assumed
8+
1500
6+
E_I (keV)
4+
1400
1300
0
20
40
60
80
k (MeV)
XBL685-2625

Fig. 14